

## SEPARATION OF MAGNETIC FIELD LINES IN TWO-COMPONENT TURBULENCE

D. RUFFOLO,<sup>1,2</sup> W. H. MATTHAEUS,<sup>3</sup> AND P. CHUYCHAI<sup>1,3</sup>

Received 2002 December 24; accepted 2004 June 18

### ABSTRACT

The problem of the separation of random magnetic field lines in collisionless astrophysical plasmas is closely related to the problem of the magnetic field line random walk and is highly relevant to the transport of charged particles in turbulent plasmas. In order to generalize treatments based on quasi-linear theory, here we examine the separation of nearby magnetic field lines by employing a nonperturbative technique based on the Corrsin independence hypothesis. Specifically, we consider the case of two-component turbulence in which the magnetic field fluctuations are a mixture of one-dimensional (slab) and two-dimensional ingredients, as a concrete example of anisotropic turbulence that provides a useful description of turbulence in the solar wind. We find that random field trajectories can separate in general through three regimes of the behavior of the running diffusion coefficient: slow diffusive separation, an intermediate regime of superdiffusion, and fast diffusive separation at large distances. These features are associated with the gradual, exponential divergence of field lines within islands of two-dimensional turbulence, followed by diffusive separation at long distances. The types of behavior are determined not by the Kubo number but rather a related ratio that takes the turbulence anisotropy into account. These results are confirmed by computer simulations. We discuss implications for space observations of energetic charged particles, including “dropouts” of solar energetic particles.

*Subject headings:* diffusion — magnetic fields — Sun: particle emission — turbulence

### 1. INTRODUCTION

The random walk of individual magnetic field lines relative to the mean magnetic field and the rate of separation of nearby field lines are key issues in defining the topology and structure of random magnetic fields in magnetohydrodynamic (MHD) turbulence. The statistics of such a random walk are often central to understanding the diffusion of energetic charged particles perpendicular to the mean magnetic field in astrophysical plasmas (Jokipii 1966; Jokipii & Parker 1968). Perpendicular diffusion is an important component of the solar cycle-dependent modulation of Galactic cosmic rays (Parker 1965; Moraal 1976; Cane et al. 1999; Reinecke et al. 2000). Determining the rate of perpendicular diffusion of energetic particles in the heliosphere may be crucial in distinguishing between two popular models for explaining the dramatic observations by the *Ulysses* spacecraft of apparent corotating interaction region (CIR) modulation of Galactic and anomalous cosmic rays (Kunow et al. 1995; McKibben et al. 1995; Simpson et al. 1995) and acceleration of low-energy electrons and ions (Sanderson et al. 1995; Simnett et al. 1995) at higher heliospheric latitudes than where CIRs were observed, i.e., the models of Kóta & Jokipii (1995) and Fisk (1996). Other issues of energetic particle transport in the heliosphere may rely on details of perpendicular diffusion, such as the poor access of Galactic cosmic rays into a coronal mass ejection (Cane et al. 1994) that can account for the deep minima of Forbush decreases, or energetic particle acceleration at a nearly perpen-

dicular shock (Jokipii 1987; Jokipii et al. 1993; Kirk et al. 1996; Jones et al. 1998).

On the other hand, there are also situations in which the behavior of distributions of energetic charged particles might be better understood in terms of the mutual separation of field lines than by the random walk of individual field lines (Jokipii 1973). Indeed, for an initially concentrated distribution of particles (assumed to be following field lines) to spread in the directions perpendicular to the mean magnetic field requires that the field lines threading the distribution mutually separate; a correlated wandering of nearby field lines would just displace the particle distribution without distorting it. Figure 1 illustrates the random walk perpendicular to the mean field ( $\Delta x$ ), the displacement between nearby field lines ( $X \equiv x_2 - x_1$ ), and their separation  $\Delta X \equiv X - X_0$ . In the extreme case in which two turbulent field lines are completely decorrelated, the mean squared separation would be twice the mean squared random walk. On the other hand, two nearby field lines could follow highly correlated trajectories with a mutual separation much lower than the displacement from the mean field, as represented by the lower two field lines in Figure 1. Therefore, field line separation is a sensitive probe of the dissimilarity of nearby field lines and the transverse structure of magnetic turbulence.

One application of calculating the field line separation is to address the long-recognized phenomenon of “channeling,” or sudden changes in the fluxes of solar energetic particles (SEPs), which has been revisited by recent, detailed measurements of Mazur et al. (2000), who refer to such events as “dropouts.” These are presumably due to sudden changes in magnetic connection to a spatially localized injection region. This picture requires that field lines that are adjacent when near the Sun remain confined to localized flux tubes out to distances  $\sim 1$  AU along the mean field.

In particular, Mazur et al. (2000) identify episodes of dramatic SEP intensity changes on an average timescale of 3 hr,

<sup>1</sup> Department of Physics, Chulalongkorn University, Bangkok 10330, Thailand; david\_ruffolo@yahoo.com, piyanate@corona.phys.sc.chula.ac.th.

<sup>2</sup> Current address: Department of Physics, Faculty of Science, Mahidol University, Rama VI Road, Bangkok 10400, Thailand.

<sup>3</sup> Bartol Research Institute, University of Delaware, Newark, DE 19716; yswm@bartol.udel.edu.

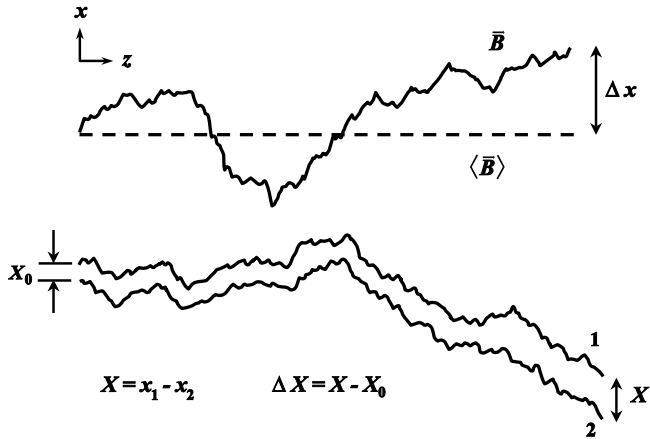


FIG. 1.—Illustration of the magnetic field line random walk perpendicular to the mean field ( $\Delta x$ ), displacement between nearby field lines ( $X \equiv x_2 - x_1$ ), and their separation ( $\Delta X \equiv X - X_0$ ). The present work calculates the mean squared separation vs. distance along the mean field.

corresponding to a spatial (longitudinal) scale of 0.03 AU. Giacalone et al. (2000) point out that if there is effectively no turbulent random walk, one can understand dropouts in terms of the field line random walk due to photospheric motions. This leads to the question, Why is there no apparent turbulent random walk? There certainly is turbulence in the interplanetary medium. One might expect a longitudinal diffusion of field lines (due to the two-dimensional component of solar wind fluctuations) to a scale of  $(\Delta x)_{\text{rms}} = (2D_{\perp}\Delta z)^{1/2}$ , where the diffusion coefficient of the turbulent random walk is  $D_{\perp} = (b/B_0)(\tilde{\lambda}/\sqrt{2})$  (Matthaeus et al. 1995) and  $\tilde{\lambda}$  is the “ultrascale” or “mesoscale,” inferred from observations to be  $\sim 0.2$  AU (Matthaeus et al. 1999). For a typical rms turbulent magnetic field of one-half the mean field,  $b = 0.5B_0$ , the expected longitudinal scale of the turbulent random walk is 0.37 AU, which would wash out the observed dropouts. One possible explanation might be that the separation of nearby field lines, which controls the spread of particles from a small injection region near the Sun, could be much slower than the turbulent random walk relative to the mean field, as illustrated in Figure 1. This issue, which is discussed again in § 6, is just one example of an astrophysical problem related to the separation of nearby magnetic field lines.

The theory of the separation of adjacent field lines has been examined by Jokipii (1973) and Zimbaro et al. (1984). This issue has been recognized as relevant to physical processes in fusion plasmas (e.g., Rechester & Rosenbluth 1978; Kadomtsev & Pogutse 1979; Isichenko 1991a, 1991b), the solar corona (e.g., Similon & Sudan 1989), energetic particle transport in the heliosphere (Erdős et al. 1997, 1999), cosmic-ray transport and acceleration in the Galaxy (Barge et al. 1984; Chandran 2000), and thermal conduction in galaxy clusters (Maron et al. 2004). Much attention has been devoted in the past to description of the exponential separation of field lines (Rechester & Rosenbluth 1978; Kadomtsev & Pogutse 1979) in the regime of small separation before the field lines undergo independent random walks, because of the relationship of that phenomenon to mixing in ergodic theory (Zaslavsky & Chirikov 1972) and stochastic instability in general. In the present paper we are mainly concerned with regimes of diffusive behavior, although we comment on the relationship between these two views of field line separation. The length scale

along the mean field over which field lines separate by a perpendicular coherence scale is relevant to incompressible MHD turbulence (Goldreich & Sridhar 1997; Lithwick & Goldreich 2001).

Apart from the observational issues discussed above, there are also a number of theoretical issues that provide motivation for reconsidering field line separation in a “realistic” (or, at least, observationally motivated) three-dimensional model magnetic field. For example, one feature of turbulence structure that has become recognized in recent years (Jones et al. 1998) is that models that are one-dimensional (“slab”) or that admit even one ignorable coordinate give rise to pathological statistical representations of particle transport. There are also indications that the stochastic instability of field lines has a character in models having small numbers of coherent modes that contrasts strongly with its character in a continuum of incoherent modes (Rax & White 1992). It is reasonable to anticipate that such differences would affect the onset and nature of diffusion. One is cautioned, then, that some properties that emerge from the simpler models of field line separation should not be taken as rigorous, especially in the light of better understood properties from observations and turbulence simulations. An example is the rather general identification of the correlation scale with the exponential separation scale (e.g., Sagdeev et al. 1988), although this is not a well-understood relationship (Rechester & Rosenbluth 1978). Similarly, the identification of the correlation scale of magnetic fluctuations with the correlation scale of the *spatial gradients* of the fluctuations (Isichenko 1991a) is manifestly incorrect for turbulence having distinct inner and outer scales. Moreover, for homogeneous turbulence, the correlation scale of derivatives, i.e., the Taylor microscale, may differ from the fluctuation correlation scale by orders of magnitude (Batchelor 1953). This difference is at least 3 or 4 orders of magnitude in the solar wind (Matthaeus & Goldstein 1982). Finally, we note that the realm of applicability of the perturbative quasi-linear (QLT) limit is often expressed (Isichenko 1991a) in terms of a dimensionless (Kubo) number  $R = (b/B_0)(\lambda_{\parallel}/\lambda_{\perp})$ , where  $\lambda_{\parallel}$  and  $\lambda_{\perp}$  are, respectively, correlation scales in the directions parallel to and perpendicular to the large-scale mean magnetic field  $B_0$ . QLT is supposed to be accurate when  $R \ll 1$ . While qualitatively correct, we can see that a criterion based solely on  $R$  cannot be complete, in view of the fact that the contribution to field line diffusion due to a quasi-two-dimensional component of the turbulence (Matthaeus et al. 1995) depends on not  $\lambda_{\perp}$  but a distinct scale (the “ultrascale”; see below) that characterizes large-scale transverse magnetic structure.

In the following sections we reexamine the theory of the separation of adjacent field lines in astrophysical MHD turbulence in light of improved understanding of solar wind turbulence in recent years (Matthaeus et al. 1990; Bieber et al. 1994). We consider field line separation in two-component turbulence consisting of a slab component that varies only along the mean field, as well as a two-dimensional component that varies only in the two transverse directions, which has been shown to serve as a useful model of solar wind turbulence (Bieber et al. 1996). This turbulence model can also be viewed as a concrete example that is representative of anisotropic turbulence in general, i.e., turbulence that varies differently along or perpendicular to the mean magnetic field. We proceed using a nonperturbative approach similar to that which has been used previously (Matthaeus et al. 1995; Gray

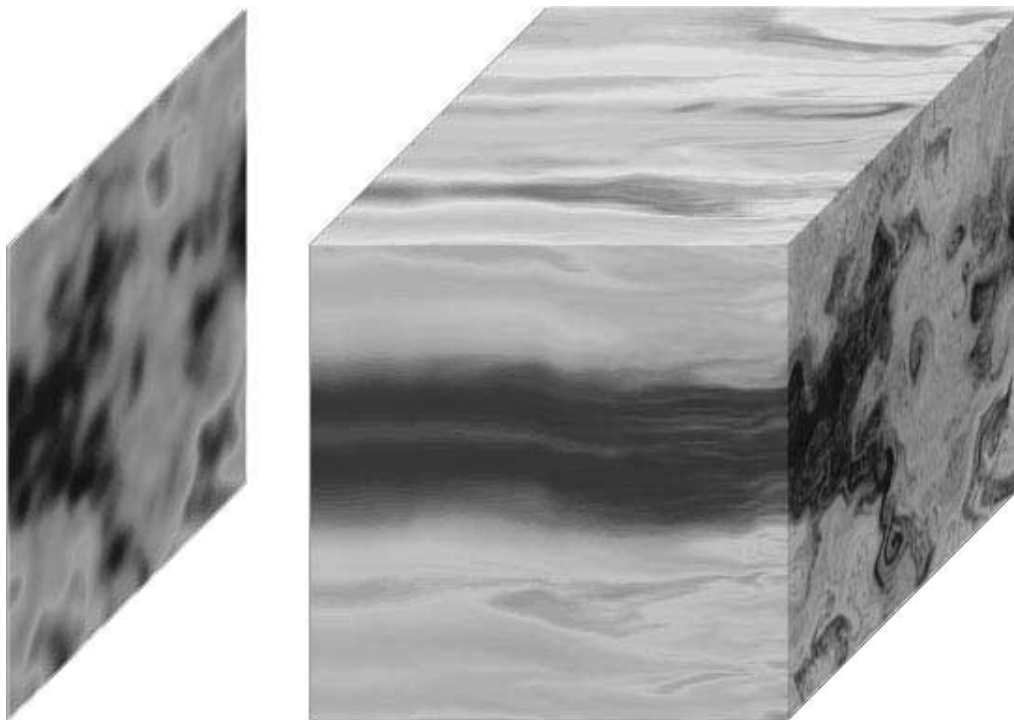


FIG. 2.—Field line motion in a realization of 2D+slab turbulence. In the left part of the figure, the shading indicates the initial value of  $a(x, y)$ , the potential function for the two-dimensional component. In the right part, that initial shading is convected along random field lines. The mean field direction,  $\hat{z}$ , is to the right. It can be seen that some regions exhibit strong mixing, while others are still organized as distinct flux tubes.

et al. 1996) to examine the field line random walk. The analytic results are verified by computer simulations. We then consider their astrophysical implications.

## 2. 2D+SLAB TURBULENCE

In the 2D+slab model of magnetic turbulence, we assume

$$\mathbf{B} = \mathbf{B}_0 + \mathbf{b}(x, y, z), \quad (1)$$

where the mean field  $\mathbf{B}_0$  is constant. We also use

$$\mathbf{B}_0 = B_0 \hat{z}, \quad \mathbf{b} \perp \hat{z}, \quad (2)$$

and the fluctuating field, of mean zero, is given by

$$\mathbf{b} = \mathbf{b}^{2D}(x, y) + \mathbf{b}^{\text{slab}}(z). \quad (3)$$

For brevity, we refer to a quantity such as  $\langle b^2 \rangle$  as the magnetic energy of the fluctuations. In general, we can write

$$\mathbf{b}^{2D}(x, y) = \nabla \times [a(x, y) \hat{z}], \quad (4)$$

where  $a\hat{z}$  can be interpreted as a vector potential for the two-dimensional component of turbulence or as a poloidal (transverse) flux function, in the sense that  $\int_1^2 \mathbf{b}^{2D} \cdot \hat{\mathbf{n}} d\ell = a(2) - a(1)$ , where  $d\ell$  is the line element along any curve connecting points 1 and 2 and  $\hat{\mathbf{n}}$  is the two-dimensional normal to that curve. Note that any large-scale gradient in  $a$  would violate the assumption that the mean magnetic field is uniform and along the  $\hat{z}$ -direction. Thus,  $a(x, y)$  can be viewed as a random function, fluctuating about a constant mean value, taken to be zero for convenience, with a well-behaved power spectrum  $A(k_x, k_y)$ .

This form of magnetic turbulence was motivated by an analysis of magnetic fluctuations in the solar wind (Matthaeus et al. 1990). Note that with  $\mathbf{b} \perp \hat{z}$ , we have  $B_z \equiv B_0$ , so in this model it is impossible for a magnetic field line to backtrack in the  $z$ -direction, and the  $z$ -coordinate uniquely specifies a point on a magnetic field line. This permits a direct analogy between the perpendicular motion of a magnetic field line versus  $z$  and the trajectory of a fluid element in incompressible, two-dimensional fluid dynamics versus time.

Figure 2 illustrates the flux function  $a(x, y)$  and the motion of field lines for a realization of such 2D+slab turbulence with an 80:20 ratio of two-dimensional to slab component energies, as found in the solar wind (Bieber et al. 1994, 1996). In the absence of a slab component, the 2D-turbulent field lines would move along curves of constant  $a$ , since equation (4) indicates that  $\mathbf{b}^{2D} \perp \nabla a$ . (This is analogous to Hamiltonian flow, upon the substitutions  $a \rightarrow H$  and  $z \rightarrow t$ .) In three dimensions, such field lines are constrained to flux tubes that are “cylinders” in the mathematical sense of surfaces of constant  $a(x, y)$ . What makes 2D+slab turbulence interesting is that the slab component imposes random perturbations on the field line motion, leading to mixing of field lines and wandering to regions of different  $a(x, y)$  (see also Matthaeus et al. 1995). This is illustrated in Figure 2, where the left panel shows an initial shading according to a realization of  $a(x, y)$  and the right panel shows how that shading is convected along random field lines (the distance  $z$  along the mean field increases to the right). In the absence of slab turbulence, the shading would be constant with  $z$  as field lines stick to the same value of  $a$ . In contrast, Figure 2 illustrates how the slab turbulence “mixes” field lines of different initial  $a$ -values. It is interesting that some regions exhibit strong mixing and spreading, while in others the initial shading is clearly visible in the same location, indicating that a flux tube structure is maintained over this

distance, a phenomenon that is discussed further by Ruffolo et al. (2003).

### 3. RANDOM WALK OF A SINGLE FIELD LINE

It is instructive to first review the diffusive random walk of a single magnetic field line in the 2D+slab model of turbulence. While yielding the same result as Matthaeus et al. (1995) in the long-distance limit, the present calculation allows us to determine its range of applicability and employs a different form of Corrsin's hypothesis, which we also use in the calculation of field line separation.

Following Jokipii & Parker (1969) and Jokipii (1973), we start with the defining equation of a magnetic field line,

$$\frac{dx}{B_x} = \frac{dy}{B_y} = \frac{dz}{B_z}, \quad (5)$$

and express the change in, say, the  $x$ -coordinate of a field line over a distance  $\Delta z$  along the mean magnetic field as

$$\Delta x \equiv x(\Delta z) - x(0) = \frac{1}{B_0} \int_0^{\Delta z} b_x[x(z'), y(z'), z'] dz'. \quad (6)$$

This quantity is illustrated in Figure 1. The ensemble average of  $(\Delta x)^2$  is then given by

$$\begin{aligned} \langle \Delta x^2 \rangle &= \frac{1}{B_0^2} \int_0^{\Delta z} \int_0^{\Delta z} \langle b_x[x(z'), y(z'), z'] \\ &\quad \times b_x[x(z''), y(z''), z''] \rangle dz' dz'' \\ &= \frac{1}{B_0^2} \int_0^{\Delta z} \int_0^{\Delta z} \langle b_x(x', y', z') b_x(x'', y'', z'') \rangle dz' dz'', \quad (7) \end{aligned}$$

where we introduce the notation  $x'$  for  $x(z')$ , etc. We can also write

$$\begin{aligned} \langle \Delta x^2 \rangle &= \frac{1}{B_0^2} \int_0^{\Delta z} \int_{-z'}^{\Delta z - z'} \langle b_x(x', y', z') \\ &\quad \times b_x(x'', y'', z' + \Delta z') \rangle d\Delta z' dz', \quad (8) \end{aligned}$$

where  $\Delta z' \equiv z'' - z'$ , and with the assumption of homogeneity,

$$\begin{aligned} \langle \Delta x^2 \rangle &= \frac{1}{B_0^2} \int_0^{\Delta z} \int_{-z'}^{\Delta z - z'} \langle b_x(0, 0, 0) \\ &\quad \times b_x(\Delta x', \Delta y', \Delta z') \rangle d\Delta z' dz', \quad (9) \end{aligned}$$

where  $\Delta x' \equiv x'' - x'$  and  $\Delta y' \equiv y'' - y'$ . This equation describes the random walk of a single field line, and the quantities  $z'$ ,  $z''$ ,  $\Delta z'$ , and  $\Delta x'$  are illustrated in Figure 3.

Before proceeding further with the mathematical derivation, it is interesting to motivate the Matthaeus et al. (1995) result. Physically, a random walk should give diffusive behavior, with

$$\langle \Delta x^2 \rangle = 2D_{\perp} \Delta z, \quad (10)$$

$$D_{\perp} \sim \left\langle (dx/dz)^2 \right\rangle \ell \sim \frac{\langle b_x^2 \rangle}{B_0^2} \ell, \quad (11)$$

for a ‘‘mean free distance’’  $\ell$ . In terms of equation (9),  $b_x$  at  $z'$  and  $z''$  decorrelate over some distance  $\Delta z' \sim \ell$ , so the inner integral is of order  $2\langle b_x^2 \rangle \ell$ , the outer integral of order  $2\langle b_x^2 \rangle \ell \Delta z$ ,

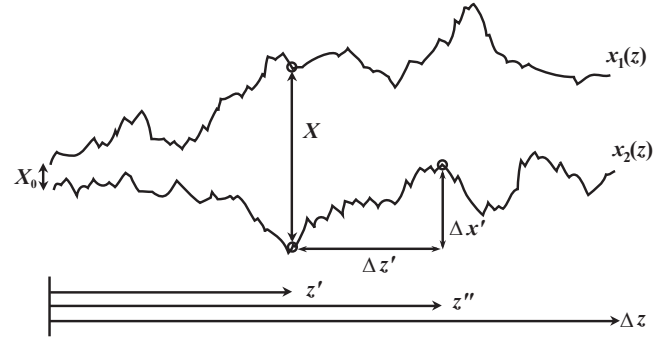


FIG. 3.—Schematic of two random field lines and definition of various quantities.

and the diffusion coefficient as given above. For slab turbulence, one might estimate  $\ell$  to be the correlation length  $\ell_c$ :

$$D_{\perp}^{\text{slab}} \sim \frac{\langle b_x^2 \rangle}{B_0^2} \ell_c, \quad (12)$$

a well-known result to be derived shortly in detail. For two-dimensional turbulence, decorrelation takes place for  $\langle \Delta x^2 \rangle \sim \tilde{\lambda}^2$ , at some perpendicular distance  $\tilde{\lambda}$ , which Matthaeus et al. (1995) refer to as the ‘‘ultrascale’’ (to be precisely defined later, in eq. [37]). Then

$$\ell \sim \frac{\tilde{\lambda}^2}{2D_{\perp}}, \quad D_{\perp} \sim \frac{\langle b^2 \rangle}{B_0^2} \frac{\tilde{\lambda}^2}{2D_{\perp}} \quad (13)$$

which has an interesting implicit form. This leads to

$$D_{\perp}^{2D} \sim \frac{\tilde{\lambda}}{\sqrt{2}} \frac{\sqrt{\langle b^2 \rangle}}{B_0}, \quad (14)$$

which depends on the rms level of fluctuation instead of the mean square. From the detailed mathematical derivation, it is seen that the ultrascale  $\tilde{\lambda}$  can be identified with the mean squared fluctuation of  $a(x, y)$  divided by that of  $\mathbf{b}^{2D}(x, y)$ . Note that this result (eq. [14]) refers to two-component turbulence in the limit of vanishing slab fluctuations. This limit is singular because for pure two-dimensional turbulence, field lines on closed flux surfaces remain confined and formally do not undergo diffusion.

Continuing with the derivation, note that Lagrangian correlation functions such as  $\langle b_x(x', y', z') b_x(x'', y'', z'') \rangle$  differ from standard (Eulerian) correlation functions; in a Lagrangian ensemble average over representations of the magnetic turbulence, the positions themselves depend on the representation. However, it is possible to separate the statistics of the magnetic fluctuations from those of individual trajectories when the two positions are displaced by more than a coherence length in the parallel or perpendicular direction. (Over smaller distances this is not necessarily accurate, e.g., straight line trajectories, with one spatial distribution, are associated with higher magnetic correlation than bending trajectories, which have a different spatial distribution.) This approximation, known as Corrsin's independence hypothesis (Corrsin 1959; Salu & Montgomery 1977; see also McComb 1990) can be expressed either in wave-vector space (as in Matthaeus et al. 1995) or in position space. Computer simulations have been used to verify the hypothesis for the random walk calculation (Gray et al. 1996) and are also used to verify its validity in the present work.

Here we demonstrate the implementation of Corrsin's hypothesis in position space. We consider the Lagrangian correlation function to be the Eulerian correlation function,  $R_{xx} \equiv \langle b_x(0, 0, 0)b_x(x, y, z) \rangle$ , weighted by the conditional probabilities of finding  $\Delta x'$  and  $\Delta y'$  after a given  $\Delta z'$ :

$$\begin{aligned} & \langle b_x(0, 0, 0)b_x(\Delta x'(\Delta z'), \Delta y'(\Delta z'), \Delta z') \rangle \\ &= \int_{-\infty}^{\infty} \int_{-\infty}^{\infty} R_{xx}(\Delta x', \Delta y', \Delta z') \\ & \quad \times P(\Delta x'|\Delta z')P(\Delta y'|\Delta z') d\Delta x' d\Delta y', \end{aligned} \quad (15)$$

$$\begin{aligned} \langle \Delta x^2 \rangle &= \frac{1}{B_0^2} \int_0^{\Delta z} \int_{-z'}^{\Delta z-z'} \int_{-\infty}^{\infty} \int_{-\infty}^{\infty} R_{xx}(\Delta x', \Delta y', \Delta z') \\ & \quad \times P(\Delta x'|\Delta z')P(\Delta y'|\Delta z') d\Delta x' d\Delta y' d\Delta z' dz', \end{aligned} \quad (16)$$

where we invoke the statistical independence of  $\Delta x'$  and  $\Delta y'$ .

Another key assumption is that the conditional probability distributions are Gaussian,

$$\begin{aligned} P(\Delta x'|\Delta z') &= \frac{1}{\sqrt{2\pi\sigma_x^2}} \exp\left[-\frac{(\Delta x')^2}{2\sigma_x^2}\right], \\ P(\Delta y'|\Delta z') &= \frac{1}{\sqrt{2\pi\sigma_y^2}} \exp\left[-\frac{(\Delta y')^2}{2\sigma_y^2}\right]. \end{aligned} \quad (17)$$

Furthermore, we assume that the variances  $\sigma_x^2 = \langle \Delta x^2 \rangle$  and  $\sigma_y^2 = \langle \Delta y^2 \rangle$  are diffusive and statistically axisymmetric in the sense that

$$\langle \Delta x^2 \rangle = \langle \Delta y^2 \rangle = 2D_{\perp}|\Delta z'|, \quad (18)$$

where  $D_{\perp}$  is the desired perpendicular diffusion coefficient. The distributions in equation (17) guarantee the statistical independence assumed in equation (16). For slab or two-component turbulence, these assumptions are accurate for sufficiently large  $\Delta z$ , by the central limit theorem. A check on the validity of the result is that  $\langle \Delta x^2 \rangle$  should be proportional to  $\Delta z$  in that limit, and as  $\Delta z$  decreases, violation of that proportionality indicates the limit of validity of the diffusion approximation. For example, at small  $\Delta z$ , over which  $\mathbf{b}$  is nearly constant, there is a "free-streaming" regime in which field lines have nearly straight-line trajectories and  $\langle \Delta x^2 \rangle \propto (\Delta z)^2$ .

So far, our calculation of  $\langle \Delta x^2 \rangle$  has not yet specified the nature of the magnetic turbulence. Now let us focus on axisymmetric, two-component 2D+slab turbulence (eqs. [1]–[3]):

$$R_{xx}(\Delta x', \Delta y', \Delta z') = R_{xx}^{\text{slab}}(\Delta z') + R_{xx}^{2D}(\Delta x', \Delta y'), \quad (19)$$

or in terms of power spectra,

$$\begin{aligned} R_{xx}^{\text{slab}}(\Delta z') &= \frac{1}{\sqrt{2\pi}} \int_{-\infty}^{\infty} P_{xx}^{\text{slab}}(k_z) e^{-ik_z \Delta z'} dk_z, \\ R_{xx}^{2D}(\Delta x', \Delta y') &= \frac{1}{2\pi} \int_{-\infty}^{\infty} \int_{-\infty}^{\infty} P_{xx}^{2D}(k_x, k_y) e^{-ik_x \Delta x'} \\ & \quad \times e^{-ik_y \Delta y'} dk_x dk_y. \end{aligned} \quad (20)$$

Then, substituting equations (19) and (20) into equation (16) and separating slab and two-dimensional contributions, we have

$$\begin{aligned} \langle \Delta x^2 \rangle_{\text{slab}} &= \\ & \frac{1}{\sqrt{2\pi}} \frac{1}{B_0^2} \int_{-\infty}^{\infty} P_{xx}^{\text{slab}}(k_z) \int_0^{\Delta z} \int_{-z'}^{\Delta z-z'} \left[ \int_{-\infty}^{\infty} P(\Delta x'|\Delta z') d\Delta x' \right] \\ & \times \left[ \int_{-\infty}^{\infty} P(\Delta y'|\Delta z') d\Delta y' \right] e^{-ik_z \Delta z'} d\Delta z' dz' dk_z, \end{aligned} \quad (21)$$

$$\begin{aligned} \langle \Delta x^2 \rangle_{2D} &= \frac{1}{2\pi} \frac{1}{B_0^2} \int_{-\infty}^{\infty} \int_{-\infty}^{\infty} P_{xx}^{2D}(k_x, k_y) \\ & \quad \times \int_0^{\Delta z} \int_{-z'}^{\Delta z-z'} \left[ \int_{-\infty}^{\infty} e^{-ik_x \Delta x'} P(\Delta x'|\Delta z') d\Delta x' \right] \\ & \quad \times \left[ \int_{-\infty}^{\infty} e^{-ik_y \Delta y'} P(\Delta y'|\Delta z') d\Delta y' \right] d\Delta z' dz' dk_x dk_y. \end{aligned} \quad (22)$$

For the slab component of turbulence, in which  $R_{xx}^{\text{slab}}$  does not depend on  $\Delta x'$  or  $\Delta y'$ , the conditional probabilities simply integrate to 1, yielding

$$\begin{aligned} \langle \Delta x^2 \rangle_{\text{slab}} &= \frac{1}{\sqrt{2\pi}} \frac{1}{B_0^2} \\ & \quad \times \int_{-\infty}^{\infty} \int_0^{\Delta z} \int_{-z'}^{\Delta z-z'} P_{xx}^{\text{slab}}(k_z) e^{-ik_z \Delta z'} d\Delta z' dz' dk_z. \end{aligned} \quad (23)$$

For the two-dimensional component, we have

$$\begin{aligned} & \int_{-\infty}^{\infty} e^{-ik_x \Delta x'} P(\Delta x'|\Delta z') d\Delta x' \\ &= \int_{-\infty}^{\infty} \frac{e^{-ik_x \Delta x'}}{\sqrt{4\pi D_{\perp} |\Delta z'|}} \exp\left[-\frac{(\Delta x')^2}{4D_{\perp} |\Delta z'|}\right] d\Delta x' \\ &= e^{-D_{\perp} k_x^2 |\Delta z'|}, \end{aligned} \quad (24)$$

and with the analogous formula for the  $\Delta y'$  integral, we obtain

$$\begin{aligned} \langle \Delta x^2 \rangle_{2D} &= \frac{1}{2\pi} \frac{1}{B_0^2} \int_{-\infty}^{\infty} \int_{-\infty}^{\infty} \int_0^{\Delta z} \int_{-z'}^{\Delta z-z'} P_{xx}^{2D}(k_x, k_y) \\ & \quad \times e^{-D_{\perp} (k_x^2 + k_y^2) |\Delta z'|} d\Delta z' dz' dk_x dk_y. \end{aligned} \quad (25)$$

So far this derivation is equivalent to that of Matthaeus et al. (1995), except that we consider the exact limits of the  $\Delta z'$  integration, not approximating the limits as  $\pm\infty$ .

Now we may carry out the integration over  $\Delta z'$  and  $z'$  in equations (23) and (25), to obtain

$$\langle \Delta x^2 \rangle_{\text{slab}} = \frac{1}{\sqrt{2\pi}} \frac{1}{B_0^2} \int_{-\infty}^{\infty} \frac{2[1 - \cos(k_z \Delta z)]}{k_z^2} P_{xx}^{\text{slab}}(k_z) dk_z, \quad (26)$$

$$\begin{aligned} \langle \Delta x^2 \rangle_{2D} &= \frac{1}{2\pi} \frac{1}{B_0^2} \int_{-\infty}^{\infty} \int_{-\infty}^{\infty} \frac{2\Delta z P_{xx}^{2D}(k_x, k_y)}{D_{\perp} (k_x^2 + k_y^2)} \\ & \quad \times \left[ 1 + \frac{e^{-D_{\perp} (k_x^2 + k_y^2) \Delta z} - 1}{D_{\perp} (k_x^2 + k_y^2) \Delta z} \right] dk_x dk_y \\ &= \frac{1}{2\pi} \frac{1}{B_0^2} \frac{2\Delta z}{D_{\perp}} \int_{-\infty}^{\infty} \int_{-\infty}^{\infty} \frac{P_{xx}^{2D}(k_x, k_y)}{k_{\perp}^2} \\ & \quad \times [1 - g(D_{\perp} k_{\perp}^2 \Delta z)] dk_x dk_y, \end{aligned} \quad (27)$$

where  $k_{\perp}^2 \equiv k_x^2 + k_y^2$ , and  $g(u) \equiv (1 - e^{-u})/u$  behaves as a low-pass filter; i.e.,  $g(u) \approx 1$  for  $u \ll 1$  and monotonically declines to zero as  $u \rightarrow \infty$ . We then obtain an expression for the perpendicular diffusion coefficient for a single field line,  $D_{\perp} \equiv \langle \Delta x^2 \rangle / (2\Delta z)$ :

$$D_{\perp} = \frac{1}{\sqrt{2\pi}} \frac{1}{B_0^2} \int_{-\infty}^{\infty} \frac{[1 - \cos(k_z \Delta z)]}{k_z^2 \Delta z} P_{xx}^{\text{slab}}(k_z) dk_z + \frac{1}{2\pi} \frac{1}{B_0^2} \frac{1}{D_{\perp}} \times \int_{-\infty}^{\infty} \int_{-\infty}^{\infty} \frac{P_{xx}^{2D}(k_x, k_y)}{k_{\perp}^2} [1 - g(D_{\perp} k_{\perp}^2 \Delta z)] dk_x dk_y. \quad (28)$$

Note that this formula is implicit in the sense that  $D_{\perp}$  appears on both sides of the equation and nonperturbative in the sense that it applies for any  $P_{xx}^{\text{slab}}$  and  $P_{xx}^{2D}$ . Note also that a diffusion coefficient is a valid concept only when  $\langle \Delta x^2 \rangle \propto \Delta z$ , i.e., when this expression for  $D_{\perp}$  is constant in  $\Delta z$ . Next, we show that this is indeed the case for sufficiently large  $\Delta z$ .

Equation (28) can be interpreted further when we consider that most observed power spectra of magnetic turbulence have power concentrated below and in the vicinity of a certain scale  $k_0$ , which is associated with a coherence scale  $\ell = 1/k_0$ . Now if there is no two-dimensional component, we have

$$D_{\perp}^{\text{slab}} = \frac{1}{\sqrt{2\pi}} \frac{1}{B_0^2} \int_{-\infty}^{\infty} \frac{[1 - \cos(k_z \Delta z)]}{k_z^2 \Delta z} P_{xx}^{\text{slab}}(k_z) dk_z. \quad (29)$$

Note that as  $\Delta z \rightarrow \infty$ ,

$$\frac{1 - \cos(k_z \Delta z)}{k_z^2 \Delta z} \rightarrow \pi \delta(k_z) \quad (30)$$

and

$$D_{\perp}^{\text{slab}} = \sqrt{\frac{\pi}{2}} \frac{P_{xx}^{\text{slab}}(0)}{B_0^2}. \quad (31)$$

This dependence, originally derived by Jokipii & Parker (1968), is approximately true for large  $\Delta z$ , i.e.,  $\Delta z \gg \ell_z = 1/k_{0z}$ , where  $\ell_z$  is a parallel coherence length, provided that  $P_{xx}^{\text{slab}}$  is roughly constant for  $k_z \ll k_{0z}$ . Equation (31) can also be expressed as

$$D_{\perp}^{\text{slab}} = \frac{\langle b_x^2 \rangle^{\text{slab}}}{B_0^2} \ell_c \quad (32)$$

for the correlation length  $\ell_c$ , as physically motivated earlier (eq. [12]).

Next, considering the limit of vanishing slab turbulence, we have  $D_{\perp} = D_{\perp}^{2D}$ , and

$$(D_{\perp}^{2D})^2 = \frac{1}{2\pi} \frac{1}{B_0^2} \int_{-\infty}^{\infty} \int_{-\infty}^{\infty} \frac{P_{xx}^{2D}(k_x, k_y)}{k_{\perp}^2} \times [1 - g(D_{\perp} k_{\perp}^2 \Delta z)] dk_x dk_y. \quad (33)$$

(A note on notation:  $D_{\perp}^{2D}$  refers to the perpendicular random walk in the limit of no slab turbulence, while  $\langle \Delta x^2 \rangle_{2D}$  refers to the contribution of two-dimensional turbulence even if slab turbulence is present.) Since  $g$  acts as a low-pass filter,  $1 - g$  acts as a high-pass filter, which is close to 1 except that it becomes small within a ‘‘hole’’ in  $(k_x, k_y)$  space, for  $k_{\perp} \lesssim [1/(D_{\perp} \Delta z)]^{1/2}$ . As  $\Delta z \rightarrow \infty$ , the width of this hole decreases, and our expression for  $D_{\perp}^{2D}$  is equivalent to that of Matthaeus

et al. (1995). The effect of the hole around  $k_{\perp} = 0$  is negligible if its size is much smaller than  $k_{0\perp}$ , so the expression

$$D_{\perp}^{2D} = \sqrt{\frac{1}{2\pi} \frac{1}{B_0^2} \int_{-\infty}^{\infty} \int_{-\infty}^{\infty} \frac{P_{xx}^{2D}(k_x, k_y)}{k_{\perp}^2} dk_x dk_y} \quad (34)$$

is valid for  $k_{0\perp}^2 D_{\perp} \Delta z \gg 1$ , i.e.,  $\langle \Delta x^2 \rangle \gg \ell_{\perp}$ , for perpendicular excursions greater than the scale  $\ell_{\perp} = 1/k_{0\perp}$ . Referring to the flux function (vector potential)  $a(x, y)$  for the two-dimensional turbulence (see § 2), we have

$$P_{xx}^{2D}(k_x, k_y) = k_y^2 A(k_{\perp}) \quad \text{and} \quad P_{yy}^{2D}(k_x, k_y) = k_x^2 A(k_{\perp}), \quad (35)$$

where  $A(k_{\perp})$ , the (axisymmetric) power spectrum of  $a(x, y)$ , is defined as the Fourier transform of the correlation function  $\langle a(0, 0)a(x, y) \rangle$ . Then  $P_{xx}^{2D} + P_{yy}^{2D} = k_{\perp}^2 A$ , and assuming axisymmetry, the integral of  $P_{xx}^{2D}/k_{\perp}^2$  is one-half that of  $A$ . Thus, we can relate  $D_{\perp}^{2D}$  to the variance of  $a(x, y)$ :

$$D_{\perp}^{2D} = \sqrt{\frac{1}{2\pi} \frac{1}{2B_0^2} \int_{-\infty}^{\infty} \int_{-\infty}^{\infty} A(k_{\perp}) dk_x dk_y} = \sqrt{\frac{\langle a^2 \rangle}{2B_0^2}}, \quad (36)$$

and finally we can define the ‘‘ultrascale’’

$$\tilde{\lambda} \equiv \sqrt{\frac{\langle a^2 \rangle}{\langle b^2 \rangle^{2D}}}, \quad (37)$$

again yielding a form that was physically motivated earlier (eq. [14]):

$$D_{\perp}^{2D} = \frac{\tilde{\lambda}}{\sqrt{2}} \frac{\sqrt{\langle b^2 \rangle^{2D}}}{B_0}. \quad (38)$$

By way of an analogy with hydrodynamic correlation functions (Batchelor 1953), we see that  $\tilde{\lambda}$  is the length associated with the curvature of the  $\langle aa' \rangle$  correlation at zero separation (see eq. [37]) and therefore may be thought of as the Taylor microscale, or ‘‘inner scale,’’ of the  $\langle aa' \rangle$  correlation function.

In summary, substituting equations (29) and (33) into equation (28) gives

$$D_{\perp} = D_{\perp}^{\text{slab}} + \frac{(D_{\perp}^{2D})^2}{D_{\perp}},$$

$$D_{\perp} = \frac{D_{\perp}^{\text{slab}}}{2} + \sqrt{\left(\frac{D_{\perp}^{\text{slab}}}{2}\right)^2 + (D_{\perp}^{2D})^2}, \quad (39)$$

for  $D_{\perp}^{\text{slab}}$  and  $D_{\perp}^{2D}$  as in equations (32) and (38), respectively (Matthaeus et al. 1995). We recall that this derivation assumes a diffusive random walk of the field line, which is valid only in the regime where  $\langle \Delta x^2 \rangle \propto \Delta z$ . This is true of the results for large  $\Delta z$  as given above, and evaluating  $\langle \Delta x^2 \rangle$  on the basis of this formula for  $D_{\perp}$  verifies that the range of validity is for  $\langle \Delta x^2 \rangle^{1/2}$  and  $\Delta z$  greater than the respective coherence lengths. This built-in check of the range of validity arises from not approximating the limits of  $d\Delta z'$  integration as  $\pm\infty$ . Equation (28) agrees with previous results while also providing a built-in

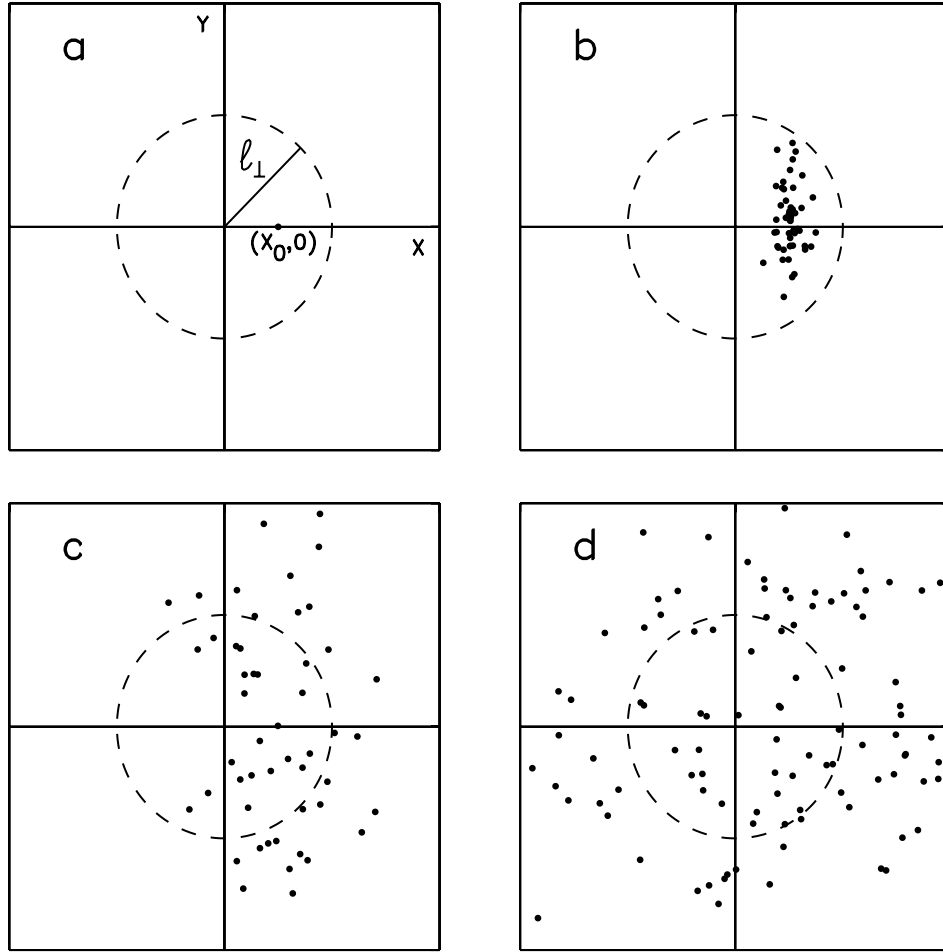


FIG. 4.—Schematic of the separation of field lines, i.e., the change in displacement  $(X, Y)$  between two field lines for a small initial displacement  $(X_0, 0)$ . (a) Two-dimensional turbulence is strongly correlated only for displacements within the dashed circle, of less than a perpendicular coherence length  $\ell_{\perp}$ . (b–d) Distribution of field line displacements with increasing  $\Delta z$ . (b) Slow diffusive separation. (c) Superdiffusive separation. (d) Fast diffusive separation.

check on the regime of validity. This is important in the following derivation of the field line separation.

#### 4. SEPARATION OF TWO FIELD LINES

##### 4.1. Mathematical Derivation

In this section, we derive the separation of two magnetic field lines in two-component 2D+slab turbulence. Now we consider the lateral coordinates of two different field lines,  $x_1(z)$ ,  $y_1(z)$ ,  $x_2(z)$ , and  $y_2(z)$ , expressing the displacement between them by  $X \equiv x_1 - x_2$  and  $Y \equiv y_1 - y_2$  (see Figs. 1 and 3). Without loss of generality, we consider  $X(z=0) = X_0$  and  $Y(z=0) = 0$ ; i.e., the  $x$ -direction is defined to be along the displacement between the two field lines at  $z=0$ . Then the separation of the field lines is expressed as the change in displacement,  $(\Delta X, \Delta Y)$ , as a function of distance  $\Delta z$  along the mean magnetic field.

Note that although the turbulence can be assumed to be statistically homogeneous and axisymmetric in position space  $(x, y)$ , the same cannot be said for displacement space  $(X, Y)$  (see Fig. 4). In particular, when one considers the correlation between the two-dimensional component of the turbulent field,  $\mathbf{b}^{2D}$ , at the positions of the two field lines, there is a fundamental difference between a distance much less than  $\ell_{\perp}$  (strong correlation) and a distance much greater than  $\ell_{\perp}$  (weak correlation). When we define the initial displacement as  $(X_0, 0)$ , then the separation in the two directions,  $\Delta X$  and  $\Delta Y$ , need not be

statistically identical, as we show mathematically in this section. Physically,  $\Delta X$  initially represents a changing distance between the two field lines, while  $\Delta Y$  initially implies a changing orientation of the displacement (Fig. 4). After a large  $\Delta z$ , when  $\langle \Delta X^2 \rangle^{1/2}$  and  $\langle \Delta Y^2 \rangle^{1/2}$  are both much greater than  $\ell_{\perp}$ , the separation becomes axisymmetric, with  $\langle \Delta X^2 \rangle^{1/2} \approx \langle \Delta Y^2 \rangle^{1/2}$ .

Let us first treat  $\Delta X$ , the  $x$ -separation between two field lines after a distance  $\Delta z$ , which can be expressed as (Jokipii 1973)

$$\Delta X = \Delta x_1 - \Delta x_2 = \frac{1}{B_0} \int_0^{\Delta z} [b_x(x'_1, y'_1, z') - b_x(x'_2, y'_2, z')] dz'. \quad (40)$$

Then we have

$$\begin{aligned} \langle \Delta X^2 \rangle &= \frac{1}{B_0^2} \int_0^{\Delta z} \int_0^{\Delta z} \langle b_x(x'_1, y'_1, z') b_x(x''_1, y''_1, z'') \rangle dz' dz'' \\ &\quad + \frac{1}{B_0^2} \int_0^{\Delta z} \int_0^{\Delta z} \langle b_x(x'_2, y'_2, z') b_x(x''_2, y''_2, z'') \rangle dz' dz'' \\ &\quad - \frac{1}{B_0^2} \int_0^{\Delta z} \int_0^{\Delta z} \langle b_x(x'_1, y'_1, z') b_x(x''_2, y''_2, z'') \rangle dz' dz'' \\ &\quad - \frac{1}{B_0^2} \int_0^{\Delta z} \int_0^{\Delta z} \langle b_x(x'_2, y'_2, z') b_x(x''_1, y''_1, z'') \rangle dz' dz''. \end{aligned} \quad (41)$$

From the symmetry of “1” and “2” indices, we have

$$\langle \Delta X^2 \rangle = 2I_{11} - 2I_{12}, \quad (42)$$

where we define

$$I_{11} = \langle \Delta x^2 \rangle = \frac{1}{B_0^2} \int_0^{\Delta z} \int_0^{\Delta z} \langle b_x(x'_1, y'_1, z') b_x(x''_1, y''_1, z'') \rangle dz' dz'', \quad (43)$$

$$I_{12} = \frac{1}{B_0^2} \int_0^{\Delta z} \int_0^{\Delta z} \langle b_x(x'_1, y'_1, z') b_x(x''_2, y''_2, z'') \rangle dz' dz''. \quad (44)$$

Since slab fluctuations are independent of  $x$ - and  $y$ -coordinates, the contributions of slab turbulence to  $I_{11}$  and  $I_{12}$  are equal. Thus, the direct slab contributions to  $\langle \Delta X^2 \rangle$  cancel, which makes sense because in pure slab turbulence the two field lines maintain a constant relative displacement at all  $z$ . This leaves us with

$$\begin{aligned} \langle \Delta X^2 \rangle &= 2\langle \Delta x^2 \rangle_{2D} \\ &\quad - \frac{2}{B_0^2} \int_0^{\Delta z} \int_0^{\Delta z} \langle b_x^{2D}(x'_1, y'_1, z') b_x^{2D}(x''_2, y''_2, z'') \rangle dz' dz''. \end{aligned} \quad (45)$$

An equation for  $\langle \Delta Y^2 \rangle$  can be obtained by the substitutions  $\Delta X \rightarrow \Delta Y$ ,  $\Delta x \rightarrow \Delta y$ , and  $b_x \rightarrow b_y$ ; with the assumption of axisymmetry in  $x$  and  $y$ , we have  $\langle \Delta x^2 \rangle = \langle \Delta y^2 \rangle$ . Note that although the direct slab contributions have cancelled, the presence of slab turbulence still affects the results in that both terms on the right-hand side of equation (45) implicitly involve the total perpendicular diffusion coefficient,  $D_\perp = \langle \Delta x^2 \rangle / (2\Delta z)$  (including the slab contribution).

The calculation of the field line separation for a given  $\Delta z$  proceeds as in § 3. With the assumption of homogeneity, and again treating  $\Delta X$  first,

$$\begin{aligned} \langle \Delta X^2 \rangle &= 2\langle \Delta x^2 \rangle_{2D} - \frac{2}{B_0^2} \int_0^{\Delta z} \int_{-z'}^{\Delta z-z'} \langle b_x^{2D}(0, 0, 0) \\ &\quad \times b_x^{2D}(\Delta x'_2 - X', \Delta y'_2 - Y', \Delta z') \rangle d\Delta z' dz'. \end{aligned} \quad (46)$$

Suppressing “2” subscripts and using the simplified notation  $X' \rightarrow X$ ,  $Y' \rightarrow Y$ , and  $z' \rightarrow z$ , we have

$$\begin{aligned} \langle \Delta X^2 \rangle &= 2\langle \Delta x^2 \rangle_{2D} - \frac{2}{B_0^2} \int_0^{\Delta z} \int_{-z}^{\Delta z-z} \langle b_x^{2D}(0, 0, 0) b_x^{2D} \\ &\quad \times (\Delta x' - X, \Delta y' - Y, \Delta z') \rangle d\Delta z' dz. \end{aligned} \quad (47)$$

Here the displacement between  $x''_2$  and  $x'_1$  is expressed in terms of displacements from a common point  $x'_2$  as shown in Figure 3. Then Corrsin’s hypothesis and the assumption of independence of  $X$  and  $Y$  displacements allow us to write

$$\begin{aligned} \langle \Delta X^2 \rangle &= 2\langle \Delta x^2 \rangle_{2D} - \frac{2}{B_0^2} \frac{1}{2\pi} \int_{-\infty}^{\infty} \int_{-\infty}^{\infty} P_{xx}^{2D}(k_x, k_y) \\ &\quad \times \left\{ \int_0^{\Delta z} \left[ \int_{-z}^{\Delta z-z} \left( \int_{-\infty}^{\infty} e^{-ik_x \Delta x'} P(\Delta x' | \Delta z') d\Delta x' \right) \right. \right. \\ &\quad \times \left. \left( \int_{-\infty}^{\infty} e^{-ik_y \Delta y'} P(\Delta y' | \Delta z') d\Delta y' \right) d\Delta z' \right] \\ &\quad \times \left[ \int_{-\infty}^{\infty} e^{ik_x X} P(X|z) dX \right] \\ &\quad \times \left. \left[ \int_{-\infty}^{\infty} e^{ik_y Y} P(Y|z) dY \right] dz \right\} dk_x dk_y. \end{aligned} \quad (48)$$

We can evaluate the three square-bracketed expressions in turn, making use of Gaussian and diffusive conditional probability distributions. In the first, the  $\Delta x'$  and  $\Delta y'$  integrals (inside parentheses) can be evaluated as in equation (24), after which the  $\Delta z'$  integral is straightforward:

$$\begin{aligned} &\int_{-z}^{\Delta z-z} \left( \int_{-\infty}^{\infty} e^{-ik_x \Delta x'} P(\Delta x' | \Delta z') d\Delta x' \right) \\ &\quad \times \left( \int_{-\infty}^{\infty} e^{-ik_y \Delta y'} P(\Delta y' | \Delta z') d\Delta y' \right) d\Delta z' \\ &= \frac{1}{D_\perp k_\perp^2} \left( 2 - e^{-D_\perp k_\perp^2 (\Delta z - z)} - e^{-D_\perp k_\perp^2 z} \right). \end{aligned} \quad (49)$$

For the second bracketed expression, we note that  $X = X_0 + \Delta X$ , where  $X_0$  is the initial displacement between the two field lines. Then

$$\begin{aligned} \int_{-\infty}^{\infty} e^{ik_x X} P(X|z) dX &= e^{ik_x X_0} \int_{-\infty}^{\infty} e^{ik_x \Delta X} P(\Delta X|z) d\Delta X \\ &= e^{ik_x X_0} e^{-D_{sx} k_x^2 z}, \end{aligned} \quad (50)$$

again making use of equation (24), where  $D_{sx} \equiv \langle \Delta X^2 \rangle / (2\Delta z)$  is the diffusion coefficient for the  $x$ -separation of two magnetic field lines. The third bracketed expression is similar:

$$\int_{-\infty}^{\infty} e^{ik_y Y} P(Y|z) dY = e^{-D_{sy} k_y^2 z}. \quad (51)$$

We note that defining the initial displacement as  $(X_0, 0)$  breaks the axisymmetry of  $\Delta X$  and  $\Delta Y$  (see also Fig. 4), so  $D_{sx}$  and  $D_{sy}$  may be distinct.

Substituting equations (27), (35), and (49)–(51) into equation (48) and performing the  $z$ -integration, we obtain a complete expression for  $\langle \Delta X^2 \rangle$ :

$$\begin{aligned} \langle \Delta X^2 \rangle &= \frac{8\Delta z^2}{\langle \Delta x^2 \rangle} \frac{1}{2\pi B_0^2} \int_{-\infty}^{\infty} \int_{-\infty}^{\infty} \frac{k_y^2 A(k_\perp)}{k_\perp^2} \left\{ 1 - g \frac{\langle \Delta x^2 \rangle k_\perp^2}{2} \right. \\ &\quad - e^{ik_x X_0} \left[ g \left( \frac{\langle \Delta X^2 \rangle k_x^2}{2} + \frac{\langle \Delta Y^2 \rangle k_y^2}{2} \right) \right. \\ &\quad - \frac{1}{2} g' \left( \frac{\langle \Delta X^2 \rangle k_x^2}{2} + \frac{\langle \Delta Y^2 \rangle k_y^2}{2}, \frac{\langle \Delta x^2 \rangle k_\perp^2}{2} \right) \\ &\quad \left. \left. - \frac{1}{2} g \left( \frac{\langle \Delta X^2 \rangle k_x^2}{2} + \frac{\langle \Delta Y^2 \rangle k_y^2}{2} + \frac{\langle \Delta x^2 \rangle k_\perp^2}{2} \right) \right] \right\} dk_x dk_y, \end{aligned} \quad (52)$$



TABLE 1  
TYPES OF SEPARATION OF TWO MAGNETIC FIELD LINES IN TWO-COMPONENT TURBULENCE

Random Walk and Separation <sup>a</sup>	Distance Range	Type of Separation
$\ell_{\perp}^2 \ll \langle \Delta x^2 \rangle$ and $\langle \Delta X^2 \rangle$ .....	Long $\Delta z$	Fast diffusive separation
$\langle \Delta X^2 \rangle \sim \ell_{\perp}^2 \ll \langle \Delta x^2 \rangle$ .....	Intermediate $\Delta z$ (only for $D_{\perp}^{2D} \ll D_{\perp}^{\text{slab}}$ )	Superdiffusive
$\langle \Delta X^2 \rangle \ll \ell_{\perp}^2 \ll \langle \Delta x^2 \rangle$ .....	Intermediate $\Delta z$ (only for $D_{\perp}^{2D} \ll D_{\perp}^{\text{slab}}$ )	Slow diffusive separation
$\langle \Delta x^2 \rangle$ and $\langle \Delta X^2 \rangle \lesssim \ell_{\perp}^2$ .....	Short $\Delta z$	Nondiffusive <sup>b</sup>

<sup>a</sup> The quantity  $\langle \Delta x^2 \rangle$  is the mean squared “random walk,” the perpendicular displacement of a single magnetic field line relative to the mean field. The quantity  $\langle \Delta X^2 \rangle$  is the mean squared separation between two magnetic field lines; see also Fig. 1.

<sup>b</sup> If  $D_{\perp}^{2D} \ll D_{\perp}^{\text{slab}}$ , nondiffusive behavior applies at a short distance  $\Delta z \lesssim \ell_z$  regardless of the magnitudes of  $\langle \Delta x^2 \rangle$  and  $\langle \Delta X^2 \rangle$ .

where  $g'(u, v) \equiv (e^{-u} - e^{-v})/(v - u)$  is a two-dimensional low-pass filter that approaches 1 when and only when both  $u \ll 1$  and  $v \ll 1$ . The analogous expression for  $\langle \Delta Y^2 \rangle$  is

$$\begin{aligned} \langle \Delta Y^2 \rangle = & \frac{8\Delta z^2}{\langle \Delta x^2 \rangle} \frac{1}{2\pi B_0^2} \int_{-\infty}^{\infty} \int_{-\infty}^{\infty} \frac{k_x^2 A(k_{\perp})}{k_{\perp}^2} \left\{ 1 - g\left(\frac{\langle \Delta x^2 \rangle k_{\perp}^2}{2}\right) \right. \\ & - e^{ik_x X_0} \left[ g\left(\frac{\langle \Delta X^2 \rangle k_x^2}{2} + \frac{\langle \Delta Y^2 \rangle k_y^2}{2}\right) \right. \\ & - \frac{1}{2} g'\left(\frac{\langle \Delta X^2 \rangle k_x^2}{2} + \frac{\langle \Delta Y^2 \rangle k_y^2}{2}, \frac{\langle \Delta x^2 \rangle k_{\perp}^2}{2}\right) \\ & \left. \left. - \frac{1}{2} g\left(\frac{\langle \Delta X^2 \rangle k_x^2}{2} + \frac{\langle \Delta Y^2 \rangle k_y^2}{2} + \frac{\langle \Delta x^2 \rangle k_{\perp}^2}{2}\right) \right] \right\} dk_x dk_y, \end{aligned} \tag{53}$$

which differs from  $\langle \Delta X^2 \rangle$  only in that  $k_y^2 A(k_{\perp})$  is replaced by  $k_x^2 A(k_{\perp})$ .

In terms of diffusion coefficients, we have

$$\begin{aligned} D_{sx} = & \frac{2}{D_{\perp}} \frac{1}{2\pi B_0^2} \int_{-\infty}^{\infty} \int_{-\infty}^{\infty} \frac{k_y^2 A(k_{\perp})}{k_{\perp}^2} \left\{ 1 - g(D_{\perp} k_{\perp}^2 \Delta z) \right. \\ & - e^{ik_x X_0} \left[ g\left(D_{sx} k_x^2 \Delta z + D_{sy} k_y^2 \Delta z\right) \right. \\ & - \frac{1}{2} g'\left(D_{sx} k_x^2 \Delta z + D_{sy} k_y^2 \Delta z, D_{\perp} k_{\perp}^2 \Delta z\right) \\ & \left. \left. - \frac{1}{2} g\left(D_{sx} k_x^2 \Delta z + D_{sy} k_y^2 \Delta z + D_{\perp} k_{\perp}^2 \Delta z\right) \right] \right\} dk_x dk_y, \end{aligned} \tag{54}$$

and

$$\begin{aligned} D_{sy} = & \frac{2}{D_{\perp}} \frac{1}{2\pi B_0^2} \int_{-\infty}^{\infty} \int_{-\infty}^{\infty} \frac{k_x^2 A(k_{\perp})}{k_{\perp}^2} \left\{ 1 - g(D_{\perp} k_{\perp}^2 \Delta z) \right. \\ & - e^{ik_x X_0} \left[ g\left(D_{sx} k_x^2 \Delta z + D_{sy} k_y^2 \Delta z\right) \right. \\ & - \frac{1}{2} g'\left(D_{sx} k_x^2 \Delta z + D_{sy} k_y^2 \Delta z, D_{\perp} k_{\perp}^2 \Delta z\right) \\ & \left. \left. - \frac{1}{2} g\left(D_{sx} k_x^2 \Delta z + D_{sy} k_y^2 \Delta z + D_{\perp} k_{\perp}^2 \Delta z\right) \right] \right\} dk_x dk_y. \end{aligned} \tag{55}$$

4.2. Interpretation: Regimes of Diffusive Separation

Fortunately, the low-pass filters  $g$  and  $g'$  facilitate the interpretation of the general behavior of the mean squared

separation between two magnetic field lines, described by  $\langle \Delta X^2 \rangle$  and  $\langle \Delta Y^2 \rangle$  as functions of distance along the mean field,  $\Delta z$ . The behavior of  $\langle \Delta X^2 \rangle$  is summarized in Table 1; that of  $\langle \Delta Y^2 \rangle$  is similar.

The interpretation presented in this section has been confirmed by numerical evaluation of equations (26), (27), (52), and (53) with the MATHEMATICA program (Wolfram Research, Inc.). Results for specific numerical examples are shown in Figures 5 and 6; see Appendix for details, including the turbulence parameters. Figure 5 shows  $\langle \Delta x^2 \rangle$  and  $\langle \Delta X^2 \rangle$  as a function of  $\Delta z$ , with a log-log scale, so diffusive behavior corresponds to lines of slope 1, with a diffusion coefficient proportional to the intercept at  $\log \Delta z = 0$ . Regimes of diffusive behavior are highlighted with solid lines. Figure 6 shows diffusion coefficients  $D_{sx}$  and  $D_{sy}$  as functions of  $\Delta z$ , so here diffusive behavior corresponds to the flat portions of the curves. We must point out that the assumptions underlying our quantitative derivation are invalid if the behavior is nondiffusive. However, we can draw the qualitative conclusion that superdiffusive behavior “connects” the two diffusive regimes in Figures 5b and 6.

The regimes of behavior of the mean squared separation are controlled by the low-pass filters  $g$  and  $g'$ . The arguments of  $g$  and  $g'$  depend on quantities such as  $\langle \Delta x^2 \rangle k_{\perp}^2$  or  $\langle \Delta X^2 \rangle k_x^2$ , and the  $k_x$  and  $k_y$  integrals are dominated by the region with  $k_{\perp} \lesssim k_{0\perp}$ , so the different regimes of behavior are defined by whether  $\langle \Delta x^2 \rangle$  and  $\langle \Delta X^2 \rangle$  are greater or less than the perpendicular coherence length squared,  $\ell_{\perp}^2 = 1/k_{0\perp}^2$ .

First, we consider the case where  $\langle \Delta x^2 \rangle \gg \ell_{\perp}^2$  and  $\langle \Delta X^2 \rangle \gg \ell_{\perp}^2$ , which occurs at long distances  $\Delta z$ . In this case, all the  $g'$ - and  $g$ -terms tend to zero, and we have

$$\begin{aligned} \langle \Delta X^2 \rangle = \langle \Delta Y^2 \rangle = & 2\langle \Delta x^2 \rangle_{2D}, \\ D_{sx} = D_{sy} = & 2 \frac{(D_{\perp}^{2D})^2}{D_{\perp}} = \frac{1}{D_{\perp}} \frac{\langle a^2 \rangle}{B_0^2} = \frac{\tilde{\lambda}^2}{D_{\perp}} \frac{\langle b^2 \rangle^{2D}}{B_0^2}. \end{aligned} \tag{56}$$

We see that in the long-distance limit, the field line separation is axisymmetric, independent of the starting displacement  $X_0$ , and diffusive with a diffusion coefficient twice as great as the two-dimensional contribution to the random walk. This behavior, which we refer to as fast diffusive separation, can be seen in the long-distance regimes of Figures 5 and 6. Note that for the case of a slab-dominated random walk ( $D_{\perp}^{\text{slab}} \gg D_{\perp}^{2D}$ ),

$$D_{sx} = D_{sy} \approx \frac{2\tilde{\lambda}^2}{\ell_c} \frac{\langle b^2 \rangle^{2D}}{\langle b^2 \rangle^{\text{slab}}}, \tag{57}$$

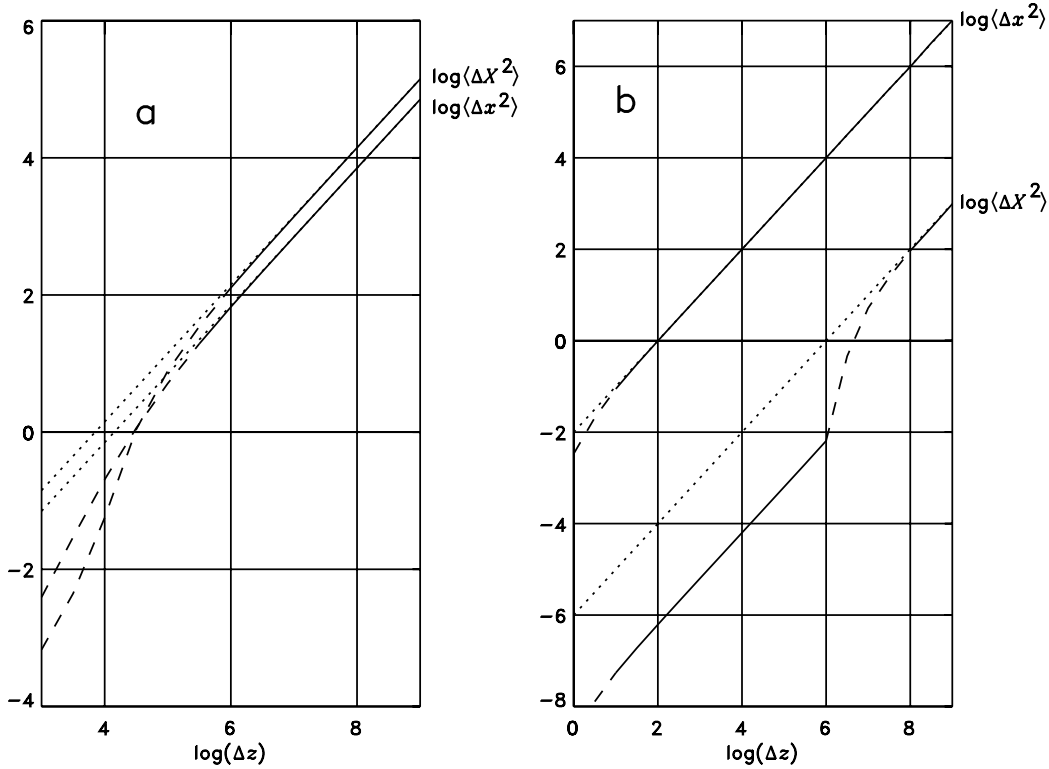


FIG. 5.—Examples of the field line random walk  $\langle \Delta x^2 \rangle$  and separation  $\langle \Delta X^2 \rangle$  as a function of  $\Delta z$ , the distance along the mean magnetic field. The random walk is dominated by (a) the two-dimensional component of turbulence, (b) the slab component of turbulence. Solid lines indicate diffusive behavior; dashed lines indicate superdiffusion. Dotted lines, for reference, show the extension of the long-distance behavior. Ordinates in units of  $\ell_\perp^2$ , abscissae in units of  $\ell_c$ . (See text for details.)

and for a two-dimensional-dominated random walk we have

$$D_{sx} = D_{sy} \approx \tilde{\lambda} \frac{\sqrt{2\langle b^2 \rangle^{2D}}}{B_0}. \quad (58)$$

To understand these results for fast diffusive separation, recall from § 1 that if two turbulent field lines were completely uncorrelated, undergoing independent random walks, the mean squared separation  $\langle \Delta X^2 \rangle$  would be twice the mean squared

random walk  $\langle \Delta x^2 \rangle$  of one field line. In the 2D+slab model of turbulence, only the two-dimensional component decorrelates in the perpendicular directions, so we can understand why the fast diffusive separation in the long-distance limit is twice as great as the two-dimensional contribution to the random walk. Since this regime involves large separations and decorrelation of the two-dimensional turbulence at the two field lines, as shown in Figure 4d, we can also understand why this behavior is axisymmetric (with  $\langle \Delta X^2 \rangle = \langle \Delta Y^2 \rangle$ ) and independent of the initial displacement between the field lines,  $X_0$ .

Paradoxically, equation (56) implies that when the slab turbulent energy  $\langle b^2 \rangle^{\text{slab}}$  is increased,  $D_\perp$  increases and the coefficient of diffusive separation *decreases* (as does the two-dimensional contribution to  $D_\perp$ ; see eq. [39]). This is illustrated by Figures 5a and 5b, which differ only in the amplitude of slab turbulence (see the Appendix for details). An interpretation of this effect is that rapid lateral excursions due to slab turbulence quickly decorrelate the “random flights” in the relative excursions of the two field lines,  $\Delta X$  and  $\Delta Y$ . The random flights depend on two-dimensional turbulence and hence  $x$  and  $y$ , which change more rapidly with increased slab turbulence. This yields a shorter mean free  $z$ -distance in the motion of one field line relative to another, hence the lower coefficient of diffusive separation.

Now let us consider what happens as  $\Delta z$  decreases. In the long-distance limit, we have fast diffusive separation where  $\langle \Delta X^2 \rangle = 2\langle \Delta x^2 \rangle_{2D}$ . In the case in which the two-dimensional component dominates the random walk,  $D_\perp^{2D} \gtrsim D_\perp^{\text{slab}}$ , we indeed have  $\langle \Delta X^2 \rangle \approx 2\langle \Delta x^2 \rangle$ . That implies that these two quantities both reach  $\ell_\perp^2$  at about the same distance  $\Delta z$  (Fig. 5a). When  $\langle \Delta x^2 \rangle \lesssim \ell_\perp^2$  and  $\langle \Delta X^2 \rangle \lesssim \ell_\perp^2$ , then the low-pass filters  $g$  and  $g'$  switch on, our expressions for  $\langle \Delta x^2 \rangle_{2D}$  and  $\langle \Delta X^2 \rangle$  instead vary

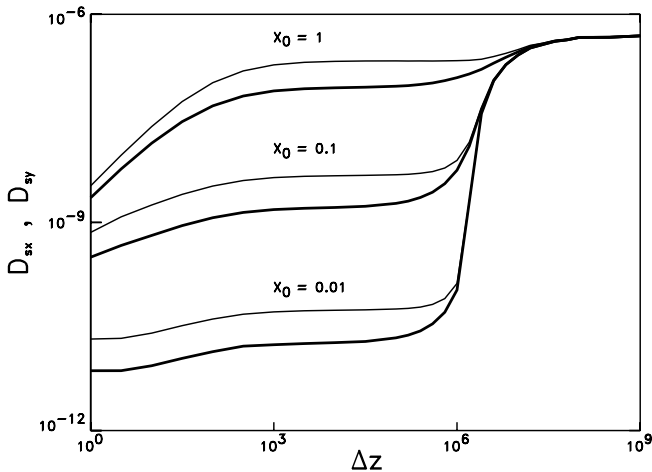


FIG. 6.—Coefficients of diffusive separation,  $D_{sx}$  (thick lines) and  $D_{sy}$  (thin lines), as a function of  $\Delta z$  for the slab-dominated case of Fig. 5b and various initial displacements  $X_0$ , with  $x$ -quantities in units of  $\ell_\perp$  and  $z$ -quantities in units of  $\ell_c$ .

as  $(\Delta z)^2$ , and our derivation is no longer valid in this regime. This indeed happens at short distances  $\Delta z$  even if the two-dimensional component does not dominate the random walk. Physically, we expect such behavior in the “free-streaming” limit where  $\mathbf{b}$  is nearly unchanged in direction. Such non-diffusive behavior, the last case listed in Table 1, can be seen at low  $\Delta z$  in Figures 5 and 6.

Therefore, when the two-dimensional component dominates the random walk, the two quantities  $\langle \Delta X^2 \rangle$  and  $\langle \Delta x^2 \rangle$  are of the same order of magnitude. On the other hand, if the slab component dominates the random walk, we can have the field line random walk much greater than the field line separation because the slab fluctuations directly contribute to the former but not the latter. Furthermore, it is possible to have

$$\langle \Delta X^2 \rangle \ll \ell_\perp^2 \ll \langle \Delta x^2 \rangle, \quad (59)$$

which is intermediate to the short-distance and long-distance regimes described above. In this case, two nearby field lines follow highly correlated trajectories with a mutual separation much lower than the displacement from the mean field, as represented by the lower two field lines in Figure 1. We refer to this behavior as “slow diffusive separation.”

Referring to equations (52)–(55) and recalling that the integrals are dominated by  $k_\perp \lesssim k_{0\perp} = 1/\ell_\perp$ , we have  $g' \rightarrow 0$  and  $g \rightarrow 0$ , with the exception that  $g(\langle \Delta X^2 \rangle k_\perp^2 / 2) \rightarrow 1$ , so

$$D_{sx} = \frac{2}{D_\perp} \frac{1}{2\pi B_0^2} \int_{-\infty}^{\infty} \int_{-\infty}^{\infty} \frac{k_y^2 A(k_\perp)}{k_\perp^2} (1 - e^{ik_x X_0}) dk_x dk_y, \quad (60)$$

$$D_{sy} = \frac{2}{D_\perp} \frac{1}{2\pi B_0^2} \int_{-\infty}^{\infty} \int_{-\infty}^{\infty} \frac{k_x^2 A(k_\perp)}{k_\perp^2} (1 - e^{ik_x X_0}) dk_x dk_y. \quad (61)$$

Recall that  $A$  is the power spectrum of  $a(x, y)$ , i.e., the Fourier transform of the autocorrelation function  $\langle a(0, 0)a(x, y) \rangle$ . Thus, the directionally averaged coefficient of slow diffusive separation is

$$D_s \equiv \frac{D_{sx} + D_{sy}}{2} = \frac{1}{D_\perp} \frac{\langle a^2 \rangle - \langle a(0, 0)a(X_0, 0) \rangle}{B_0^2}. \quad (62)$$

This expression for  $D_s$  varies linearly with the autocorrelation of the flux function  $a$  at the initial displacement between the field lines and has a direct physical interpretation. If the field lines are initially far apart with  $X_0 \gg \ell_\perp$ , so that the correlation  $\langle a(0, 0)a(X_0, 0) \rangle \rightarrow 0$ , then we recover the expression for fast diffusive separation (eq. [56]). Physically, this refers to the separation between two field lines for uncorrelated two-dimensional turbulence (and perfectly correlated slab turbulence, at the same  $z$ -coordinate), and there is no difference from the fast diffusive separation regime. On the other hand, for  $X_0 \lesssim \ell_\perp$ , field lines are initially close together with a substantial correlation in the flux function  $a$ , and the coefficient of diffusive separation is slower in this regime.

Transforming equation (62) to obtain

$$D_s = \frac{1}{D_\perp} \frac{\langle [a(X_0, 0) - a(0, 0)]^2 \rangle}{2B_0^2}, \quad (63)$$

we see that this expression is also related to the mean squared difference between  $a$  at the positions of the two field lines. Note that  $a(X_0, 0) - a(0, 0)$  can be interpreted as  $\int_1^2 \mathbf{b}^{2D} \cdot \hat{\mathbf{n}} dl$ , where  $dl$  is the line element along any curve connecting the locations

of field lines 1 and 2 and  $\hat{\mathbf{n}}$  is the two-dimensional normal to that curve, i.e., the two-dimensional magnetic flux threading any such curve. There is an interesting similarity between this expression and equation (56) for fast diffusive separation.

Another property of slow diffusive separation is that it is nonaxisymmetric, i.e.,  $\langle \Delta Y^2 \rangle > \langle \Delta X^2 \rangle$ . Recalling that the axisymmetry is broken by defining the initial displacement as  $(X_0, 0)$ ,  $\Delta X$  initially refers to the change in the distance between the two field lines, while  $\Delta Y$  implies a changing orientation of the displacement (Fig. 4). Mathematically, in the limit of small  $X_0$  and with a transformation to polar coordinates  $(k_\perp, \varphi)$ , equations (60) and (61) become

$$D_{sx} = \frac{1}{D_\perp} \frac{X_0^2}{2\pi B_0^2} \left[ \int_0^{2\pi} \sin^2 \varphi \cos^2 \varphi d\varphi \right] \int_0^\infty k_\perp^3 A(k_\perp) dk_\perp, \\ D_{sy} = \frac{1}{D_\perp} \frac{X_0^2}{2\pi B_0^2} \left[ \int_0^{2\pi} \cos^4 \varphi d\varphi \right] \int_0^\infty k_\perp^3 A(k_\perp) dk_\perp. \quad (64)$$

The bracketed integrals are  $\frac{1}{4}\pi$  and  $\frac{3}{4}\pi$ , respectively, so for small  $X_0$  the ratio of  $\langle \Delta Y^2 \rangle$  to  $\langle \Delta X^2 \rangle$  is 3:1. Using the relation  $k_\perp^2 A = P_{xx}^{2D} + P_{yy}^{2D}$ , we have

$$D_{sx} = \frac{1}{8} \frac{1}{D_\perp} \frac{\langle b^2 \rangle^{2D}}{B_0^2} X_0^2, \\ D_{sy} = \frac{3}{8} \frac{1}{D_\perp} \frac{\langle b^2 \rangle^{2D}}{B_0^2} X_0^2, \quad (65)$$

or in terms of the correlation of  $a$ , we have

$$D_{sx} = \frac{1}{2} \frac{1}{D_\perp} \frac{\langle a^2 \rangle - \langle a(0, 0)a(X_0, 0) \rangle}{B_0^2}, \\ D_{sy} = \frac{3}{2} \frac{1}{D_\perp} \frac{\langle a^2 \rangle - \langle a(0, 0)a(X_0, 0) \rangle}{B_0^2}. \quad (66)$$

Note that when  $\langle a^2 \rangle - \langle a(0, 0)a(X_0, 0) \rangle$  is expanded in terms of  $X_0$ , odd terms vanish by symmetry and the leading term is of order  $X_0^2$ . Numerical values of  $D_{sx}$  and  $D_{sy}$  are shown in Figure 6 for various values of  $X_0$  (in units of  $\ell_\perp$ ).

Figure 4 also illustrates the transition between slow diffusive separation and fast diffusive separation for a slab-dominated random walk and for  $X_0 \lesssim \ell_\perp$ . When the two field lines are closer than  $\ell_\perp$ , the two-dimensional fluctuations are strongly correlated, leading to slow diffusive separation. The distribution of the field line separation is nonaxisymmetric, preferentially changing the direction of the displacement instead of the distance. This is related to the motion of field lines subject to two-dimensional turbulence: at any given position, two field lines are typically both rotating around the same two-dimensional “island.” The mutual random walk is suppressed by the temporary confinement of field lines within a perpendicular coherence length. When the distance is of order  $\ell_\perp$ , the two-dimensional fluctuations decorrelate and the rate of separation increases. This is a regime of superdiffusion that bridges between the slow diffusive separation and fast diffusive separation (also seen in Figs. 5 and 6). Then for distances much greater than  $\ell_\perp$  one obtains the long-distance limit of fast diffusive separation, which is axisymmetric and independent of  $X_0$ . The various regimes of field line separation of summarized in Table 1.

In Figure 6, it is seen that the onset of superdiffusive behavior occurs at a certain  $\Delta z$  value, independent of  $X_0$ . This is similar to the behavior of the mean separation versus  $z$  in Figure 2 of Maron et al. (2004). This can be understood in terms of a universal curve of  $\langle R^2 \rangle$  versus  $z$ , defined by the *Ansatz*

$$\frac{d\langle R^2 \rangle}{dz} = 4D_s(\langle R^2 \rangle). \quad (67)$$

Here the function  $D_s(\langle R^2 \rangle)$  is a running diffusion coefficient, related but not necessarily identical to the diffusion coefficient derived earlier, and  $\langle R^2 \rangle$  refers to the mean squared distance between the two field lines,

$$\langle R^2 \rangle \equiv \langle X^2 \rangle + \langle Y^2 \rangle = X_0^2 + \langle \Delta X^2 \rangle + \langle \Delta Y^2 \rangle. \quad (68)$$

The value of  $D_s(\langle R^2 \rangle)$  is set to  $D_s(X_0^2)$  from the slow diffusive separation regime (in which  $\langle \Delta X^2 + \Delta Y^2 \rangle \ll X_0^2$  and  $\langle R^2 \rangle \approx X_0^2$ ) as given by equation (62). The above *Ansatz* proposes that  $D_s$  is a function only of  $\langle R^2 \rangle$  and not a function of the details of the displacement distribution, which is particularly accurate for slow diffusive separation and the onset of superdiffusion (e.g., eq. [65] shows that  $D_s \propto X_0^2$ , so replacing  $X_0^2$  by the mean  $\langle R^2 \rangle$  leaves  $D_s$  nearly unchanged). Then the choice of  $X_0$  is viewed as the choice of a starting point ( $z_0, \langle R^2 \rangle = X_0^2$ ) along the universal curve, with  $\langle \Delta X^2 + \Delta Y^2 \rangle = \langle R^2 \rangle - X_0^2$  and  $\Delta z = z - z_0$ . This model can approximately reproduce the results in Figure 6 for slow diffusive separation and the onset of superdiffusion. In that range, using  $D_\perp \approx D_\perp^{\text{slab}}$  and from equations (32) and (65), we have

$$D_s(\langle R^2 \rangle) = \frac{\langle b^2 \rangle^{2D} \langle R^2 \rangle}{\langle b^2 \rangle^{\text{slab}} 2\ell_c}, \quad (69)$$

and solving equation (67) we obtain

$$\begin{aligned} \langle R^2 \rangle &= X_0^2 e^{\Delta z / \ell_g}, \\ \langle \Delta X^2 + \Delta Y^2 \rangle &= X_0^2 \left( e^{\Delta z / \ell_g} - 1 \right), \end{aligned} \quad (70)$$

where the exponential growth length along the mean magnetic field,

$$\ell_g = \frac{\ell_c \langle b^2 \rangle^{\text{slab}}}{2 \langle b^2 \rangle^{2D}}, \quad (71)$$

marks the end of the approximately linear dependence of  $\langle \Delta X^2 + \Delta Y^2 \rangle$  on  $\Delta z$ , i.e., the end of slow diffusive separation. In this way, the onset of superdiffusion can be viewed as part of a process of exponential growth of  $\langle R^2 \rangle$  as a function of  $z$ , which is an example of stochastic instability. The result (eq. [71]) amounts to a calculation of the Kolmogorov-Lyapunov length (Rechester & Rosenbluth 1978) for a slab-dominated two-component magnetic field turbulence mode.

## 5. COMPUTER SIMULATIONS

To confirm the conclusions of these analytic calculations, we also developed computer simulations of field line separation in 2D+slab turbulence. While the simulations inevitably involve some discretization and statistical errors, they do avoid the key assumptions of the analytic work (Corrsin's hypothesis, Gaussian probability distributions, and diffusive

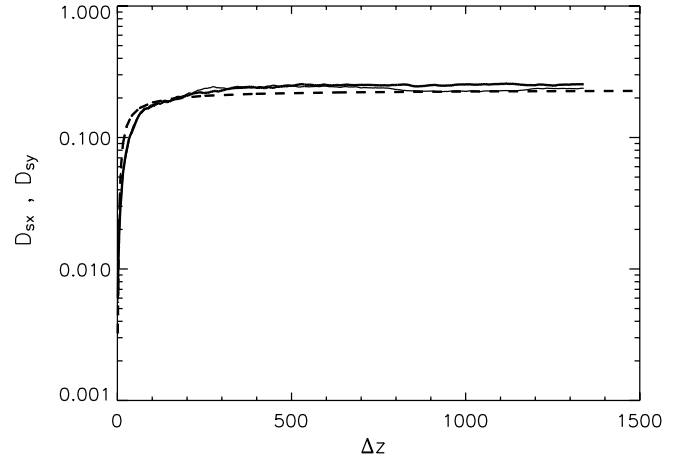


FIG. 7.—Coefficients of diffusive separation derived from computer simulations,  $D_{sx}$  (thick solid line) and  $D_{sy}$  (thin solid line), compared with  $D_{sx} = D_{sy}$  from analytic calculations (dashed line), as a function of  $\Delta z$  for a random walk dominated by the two-dimensional component of turbulence. The long-distance limit is the regime of fast diffusive separation. (See text for details.)

separation) and thus provide an independent check of their validity. Computer simulations are also useful for examining the regimes in which our analytic expressions are not valid, i.e., where the field line separation is not diffusive. The basic methods and results are presented here, and more technical details can be found in the Appendix.

The simulations involved two steps:

1. Generating representations of slab and two-dimensional turbulence with desired statistical properties, such as a power spectrum that follows the Kolmogorov power law over the inertial wavenumber range and rolls over in the energy-containing range, as observed for solar wind turbulence (Jokipii & Coleman 1968). (See the Appendix for mathematical expressions.) Random phases are used in wavenumber space, followed by inverse fast Fourier transforms to obtain  $\mathbf{b}^{\text{slab}}(z)$  and  $\mathbf{b}^{2D}(x, y)$ . The transforms in  $z$  used  $2^{23}$  ( $\approx 8.4 \times 10^6$ ) points, while the transforms in  $x$  and  $y$  used  $2^{12} = 4096$  points in each dimension.

2. Tracing magnetic field lines, i.e., solving the coupled ordinary differential equations

$$\frac{dx}{dz} = \frac{b_x(x, y, z)}{B_0}, \quad \frac{dy}{dz} = \frac{b_y(x, y, z)}{B_0}. \quad (72)$$

We used a fourth-order Runge-Kutta method with adaptive time stepping regulated by a fifth-order error estimate step (Press et al. 1992). The  $D_{sx}$  and  $D_{sy}$  values were based on averages over 1000 pairs of field lines, and each pair was for a distinct realization of slab and two-dimensional turbulence.

Now the key physical conclusions of the analytic work (Table 1) can be checked using the computer simulations. In the two-dimensional-dominated case, where  $D_\perp^{2D} \gtrsim D_\perp^{\text{slab}}$ , we expect a nondiffusive (free-streaming) regime at short  $\Delta z$ , followed by fast diffusive separation at long  $\Delta z$  (where  $\langle \Delta x^2 \rangle \gtrsim \ell_\perp^2$ ). The analytic expression is expected to hold quantitatively for diffusive behavior in the long-distance limit; in particular, the fast diffusive separation rate should be given by equation (56).

Figure 7 shows a specific example of two-dimensional-dominated behavior. Specifically, we used  $\langle b^2 \rangle^{2D} = \langle b^2 \rangle^{\text{slab}} = B_0^2/8$ ,  $X_0 = 0.1339$ , and other parameters as in the Appendix.

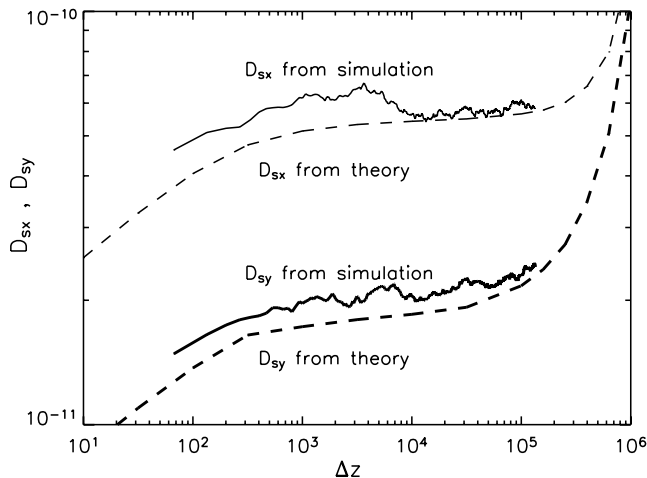


FIG. 8.—Coefficients of diffusive separation derived from computer simulations,  $D_{sx}$  (thick solid line) and  $D_{sy}$  (thin solid line), compared with those from analytic calculations (thick dashed line and thin dashed line, respectively), as a function of  $\Delta z$  for a random walk dominated by the slab component of turbulence, in the regime of slow diffusive separation. (See text for details.)

These yield  $D_{\perp}^{2D} = 0.144$  and  $D_{\perp}^{\text{slab}} = 0.0625$ . The computational box sizes were  $L_z = 10^6 \ell_z$  and  $L_x = L_y = 200 \ell_z$ . The simulation results for  $D_{sx}$  (thick solid line) and  $D_{sy}$  (thin solid line) are compared with the analytic predictions for  $D_{sx}$  and  $D_{sy}$  from equations (54) and (55), which are indistinguishable in Figure 7 (dashed line). The difference of about 10% at large  $\Delta z$  represents good quantitative agreement, given the simulation uncertainties. These include the statistical uncertainty, as estimated from the difference between simulation results for  $D_{sx}$  and  $D_{sy}$  and their stochastic variation with  $\Delta z$ , and the discretization error of about 6%, which we estimate by replacing continuous integration over  $\mathbf{k}$  in the analytic expressions with discrete sums over the  $\mathbf{k}$ -modes used in the simulations. Note also that the analytic expression correctly identifies the  $\Delta z$  range in which diffusive separation behavior begins, i.e., the lower limit of applicability of the diffusion approximation.

Another simulation with the same total turbulent energy but a 20:80 ratio of  $\langle b^2 \rangle^{\text{slab}}$  to  $\langle b^2 \rangle^{2D}$  showed a similar level of agreement. Indeed, agreement on the order of 15% was also found between computer simulations and analytic calculations for the field line random walk (Gray et al. 1996). In addition to the long-distance limit, another noteworthy feature of our two-dimensional-dominated simulations is that in the free-streaming regime, there is nonaxisymmetric separation,  $D_{sy} > D_{sx}$ , reminiscent of the analytic results in the slow diffusive regime for the slab-dominated case (see also Fig. 4).

The interesting features of analytic results for the slab-dominated case ( $D_{\perp}^{\text{slab}} \gg D_{\perp}^{2D}$ ) are a regime of nonaxisymmetric slow diffusive separation, with  $D_{sy} \approx 3D_{sx}$ , followed by a superdiffusive transition to fast diffusive separation in the long-distance limit. We performed computer simulations for the same parameter values as in Figures 5b and 6, with the exception that  $X_0$  was set to 0.01. The computational box sizes were  $L_z = 2 \times 10^6 \ell_z$  and  $L_x = L_y = 200 \ell_z$ . The comparison with analytic calculations (Fig. 8) demonstrates good agreement, with both simulation and analytic values flattening over the same range of  $\Delta z$  at the ratio  $D_{sy}/D_{sx} \approx 3$ . The difference of  $\sim 15\%$  is again of the same order as the statistical and discretization errors in the simulations (the latter is estimated

at 10%–15%) and is similar to that obtained by Gray et al. (1996).

Note that in the slab-dominated case, the slow diffusion and onset of superdiffusion can also be expressed as an exponential separation phase (see § 4.2). When fitting the computational results for  $\langle R^2 \rangle = X_0^2 + \langle \Delta X^2 \rangle + \langle \Delta Y^2 \rangle$  to an exponential function of  $z$ , we find that the best fit is for  $\langle R^2 \rangle = 9.97 \times 10^{-5} \exp(-z/6.57 \times 10^5)$ . Referring to equations (70) and (71), the analytic expectation is  $\langle R^2 \rangle = X_0^2 \exp(-z/\ell_g)$ , where for this case  $X_0^2 = 10^{-4}$  and  $\ell_g = 6.67 \times 10^5$ . Thus, the analytic and numerical calculations agree to within 0.3% for the prefactor and to within 1.5% for the exponential growth length,  $\ell_g$ .

## 6. DISCUSSION AND CONCLUSIONS

We have developed an analytic formalism for the ensemble-averaged field line random walk and separation that does not assume a long-distance limit, i.e., in which fluctuations between the two field lines have not completely decorrelated. This is possible by retaining finite limits of integration in  $\Delta z'$ . The results of the analytic theory have been confirmed by numerical simulations, justifying the use of Corrsin's hypothesis.

The analytic results we have derived are nonperturbative in the sense that neither the total turbulent energy nor the turbulent energy of the slab or the two-dimensional component is constrained to be small. The results are also not restricted to a specific functional form for the power spectrum. We consider a particular case of anisotropic turbulence, in which power in  $\mathbf{k}$ -space is concentrated along the parallel axis and (axisymmetrically) along the perpendicular plane.

With its idealized and clear separation of parallel and perpendicular fluctuations, the two-component magnetic turbulence model considered here is an archetype of highly anisotropic turbulence, which also serves as a useful model of turbulence in the solar wind (Matthaeus et al. 1990; Bieber et al. 1996) and has helped to quantitatively explain solar energetic particle transport (Bieber et al. 1994). In comparison, in the work of Jokipii (1973) all the turbulence is taken to decorrelate after a certain  $z$ -distance. In this sense it is like the slab component in our work but differs in that it also contributes to field line separation. The results of Jokipii (1973) were generalized by Zimbaro et al. (1984) to other mean field geometries.

Our overall picture of diffusive separation at long distances and nondiffusive separation at short distances, with possible regimes of slow diffusion and superdiffusion in between, is qualitatively consistent with that presented by Isichenko (1991a, 1991b) for general magnetic turbulence. As discussed in the previous section, the slow diffusion and onset of superdiffusion in the mean squared separation  $\langle \Delta X^2 + \Delta Y^2 \rangle$  can be identified as an exponential growth of the mean squared distance between two field lines,  $\langle R^2 \rangle$ , as discussed by various authors (e.g., Skilling et al. 1974; Rechester & Rosenbluth 1978; Krommes 1978; Similon & Sudan 1989; Isichenko 1991a, 1991b and references therein). It was shown by Barghouty & Jokipii (1996) that the results of Jokipii (1973) can also be interpreted in such terms. In terms of the separation of field lines, we have shown that there is a regime that can be usefully considered as diffusive and nonaxisymmetric in the perpendicular directions (slow diffusive separation; Figs. 4, 5, 6, and 8).

In our detailed work for the particular case of two-component turbulence, we find a criterion for different types of field line

separation behavior that is somewhat different from that of Isichenko (1991a, 1991b). That work, as well as Krommes (1978) and Kadomtsev & Pogutse (1979), stressed a parameter  $R$  given (in our notation) by

$$R \sim \frac{\sqrt{\langle b^2 \rangle} \ell_z}{B_0 \ell_\perp}, \quad (73)$$

sometimes called the Kubo number. On the other hand, our work identifies regimes of behavior that depend on  $D_\perp^{\text{slab}}/D_\perp^{2\text{D}}$ , the ratio of contributions to the field line random walk, which are in turn related to the amplitude of each component and the relevant distance scales. (Recall that  $D_\perp^{2\text{D}}$  contains  $\tilde{\lambda}$ , the ultrascale, which is in general distinct from the perpendicular coherence scale  $\ell_\perp$ .) Both  $D_\perp$  and  $D_s$  have different dependences for  $D_\perp^{\text{slab}}/D_\perp^{2\text{D}} \gg 1$  or  $\ll 1$  (compare eqs. [32] and [38] with eqs. [57] and [58]).

Can we reconcile the role of  $R$  in previous studies with the role of  $D_\perp^{\text{slab}}/D_\perp^{2\text{D}}$  in our work? We note that the previous work that considered  $R$  as a key parameter did not specifically consider turbulence with very different amplitudes for quasi-parallel and quasi-perpendicular wavevectors  $\mathbf{k}$ , apparently making the implicit assumption that those amplitudes are comparable. Indeed, the ratio

$$\frac{D_\perp^{\text{slab}}}{D_\perp^{2\text{D}}} = \frac{\langle b^2 \rangle^{\text{slab}}/B_0^2 \ell_c/2}{\sqrt{\langle b^2 \rangle^{2\text{D}}/B_0} \tilde{\lambda}/\sqrt{2}} \quad (74)$$

reduces to  $R$  (modulo constants of order unity) in the case where  $\langle b^2 \rangle^{\text{slab}} \sim \langle b^2 \rangle^{2\text{D}}$  and  $\tilde{\lambda} \sim \ell_\perp$ . Therefore, we suggest that the ratio of contributions to  $D_\perp$  from quasi-parallel and quasi-perpendicular wavevectors  $\mathbf{k}$  may be a more general criterion for determining the behavior of field line separation in anisotropic turbulence.

The exponential growth rate for the mean squared distance, which has also been called the Kolmogorov entropy or topological entropy (see Appendix B of Isichenko 1991b), is also found to be different for various cases of magnetic turbulence (Jokipii 1973; Barge et al. 1984; Similon & Sudan 1989; Isichenko 1991a, 1991b; Barghouty & Jokipii 1996; Maron et al. 2004), showing that general expressions are not always applicable to particular cases of interest. In our case of two-component turbulence, the exponential growth length, given by equation (71), is again related to the ratio between the amplitudes of slab and two-dimensional components of the turbulent magnetic field, not only correlation lengths and the overall amplitude as suggested by Isichenko (1991a, 1991b).

Now let us return to a specific issue raised in § 1: can observed dropouts (i.e., sharp spatial gradients) of solar

energetic particles be explained by field line separation in the solar wind that is much slower than the field line random walk? Apparently not, because observed particle motion and magnetic turbulence in the solar wind are best modeled by a roughly 80 : 20 ratio in two-dimensional : slab turbulent energy (Bieber et al. 1994, 1996), and  $\tilde{\lambda}$  is inferred from observations to be  $\sim 0.2$  AU (Matthaeus et al. 1999), so the derived value of  $D_\perp^{2\text{D}} = 0.37$  AU is about an order of magnitude higher than the slab contribution. This corresponds to a two-dimensional-dominated random walk, the case of Figure 5a, and we expect fast diffusive separation ( $D_s \approx 2D_\perp^{2\text{D}}$ ) for distances greater than a parallel coherence length of  $\sim 0.02$  AU. Therefore, field line separation should correspond to uncorrelated random walks of two field lines starting in the same region. An alternative explanation of dropouts, corresponding to temporary trapping of field lines near O-points in the turbulence, is presented by Ruffolo et al. (2003).

In conclusion, we use nonperturbative analytic techniques based on the Corrsin independence hypothesis and computer simulations to investigate the separation of magnetic field lines in a two-component model of anisotropic turbulence, which has proven to be a useful model of turbulence in the solar wind. In the long-distance limit, we predict “fast diffusive separation” with a diffusion coefficient  $D_s \approx 2(D_\perp^{2\text{D}})^2/D_\perp$ , where  $D_\perp$  refers to the perpendicular diffusion (random walk) of field lines relative to the (constant) mean magnetic field and  $D_\perp^{2\text{D}}$  is for the case of vanishing slab turbulence. This has the counterintuitive implication that increasing slab turbulence leads to a smaller  $D_s$ . If the random walk is dominated by the two-dimensional component of turbulence, fast diffusive separation begins as soon as the random walk reaches a perpendicular coherence length  $\ell_\perp$ . However, if the slab component dominates the random walk, there is more interesting behavior at intermediate  $\Delta z$ . We find nonaxisymmetric, slow diffusive separation at a rate related to the correlation of the flux function (vector potential) at the initial separation, followed by superdiffusive separation at  $\Delta z \gtrsim \ell_g$ , which increases up to the fast diffusive separation rate. The length  $\ell_g$  is identified with an exponential growth scale for the distance between neighboring magnetic field lines, which is related to the relative amplitudes of the slab and two-dimensional components.

D. R. greatly appreciates the hospitality of the Bartol Research Institute, University of Delaware, where this work was conceived. This research was partially supported by a Basic Research Grant and a Royal Golden Jubilee Fellowship from the Thailand Research Fund, the Rachadapisek Sompoj Fund of Chulalongkorn University, and the NASA Sun-Earth Connections Theory Program (grant NAG 5-8134).

## APPENDIX

### NUMERICAL EVALUATION OF ANALYTIC EXPRESSIONS

The present work yields somewhat complicated analytic expressions for the separation between two magnetic field lines in two-component turbulence (§ 4.1), which are interpreted in § 4.2. We found it useful to verify that interpretation by numerically evaluating the integrals in equations (26), (27), (54), and (55) with the MATHEMATICA program (Wolfram Research, Inc.) for some special cases. Those results, plotted in Figures 5 and 6, are found to agree with the interpretation of the analytic expressions in § 4.2. In contrast, the comparison in Figures 7 and 8 with numerical simulations, which do not incorporate the analytic theory in any way, is an independent test of the validity of the analytic theory itself and its underlying assumptions.

For the numerical evaluation of analytic expressions, the following power spectra were used:

$$P_{xx}^{\text{slab}}(k_z) = P_{yy}^{\text{slab}}(k_z) \propto \frac{1}{(1 + k_z^2/k_{0z}^2)^{5/6}}, \quad (\text{A1})$$

$$A(k_{\perp}) \propto \frac{1}{(1 + k_{\perp}^2/k_{0\perp}^2)^{7/3}}. \quad (\text{A2})$$

These forms roll off to a constant at low  $k$ , and far above  $k_{0z}$  or  $k_{0\perp}$  they follow a Kolmogorov law, with the omnidirectional power spectrum (OPS) varying as  $k^{-5/3}$ . To see this, note that for slab (one-dimensional) fluctuations the OPS is simply  $P_{xx}^{\text{slab}} + P_{yy}^{\text{slab}}$ , which has the correct dependence, and for two-dimensional fluctuations at a given magnitude  $k_{\perp}$ , the OPS  $\propto k_{\perp}(P_{xx}^{2D} + P_{yy}^{2D}) = k_{\perp}^3 A$ , which varies as  $k_{\perp}^{-5/3}$  for large  $k_{\perp}$ . However, we stress that the results described in the main text do *not* require power spectra of these specific forms.

For convenience,  $B_0$ ,  $\ell_c$ ,  $k_{0\perp}$ , and  $\ell_{\perp}$  were all set to 1. Effectively, the calculations are for  $B$  in units of  $B_0$ , and  $x$  and  $z$  in units of  $\ell_{\perp}$  and  $\ell_c$ , respectively. For the slab turbulence spectrum of equation (A1), setting  $\ell_c = 1$  implies that  $\ell_z = 1/k_{0z} = 1.339$ , and for the two-dimensional spectrum of equation (A2),  $\ell_{\perp} = 1$  implies an ultrascale  $\lambda = 0.577$ . Figure 5 used  $X_0 = 0.1$ . For Figure 5a, the slab and two-dimensional turbulence energies were set to  $\langle b^2 \rangle^{\text{slab}} = 7.07 \times 10^{-7}$  and  $\langle b^2 \rangle^{2D} = 7.5 \times 10^{-9}$ , yielding  $D_{\perp}^{\text{slab}} = 3.54 \times 10^{-7}$  and  $D_{\perp}^{2D} = 3.54 \times 10^{-5}$ , for a random walk dominated by the two-dimensional component. For Figures 5b and 6, the only difference was that the slab energy (i.e.,  $\langle b^2 \rangle^{\text{slab}}$ ) was set to 0.01, or  $1.41 \times 10^4$  times stronger, for  $D_{\perp}^{\text{slab}} = 5 \times 10^{-3}$ , so that slab turbulence dominates the random walk. These values were chosen for clarity, to separate the various physical regimes, and not to correspond to any specific physical situation such as the solar wind.

Using MATHEMATICA, we first directly calculated  $\langle \Delta x^2 \rangle_{\text{slab}}$  for various values of  $\Delta z$  and then iteratively calculated  $\langle \Delta x^2 \rangle$  and  $D_{\perp}$ . Next  $D_{xx}$  and  $D_{yy}$  were calculated iteratively and simultaneously by a secant method (using *FindRoot*). Care was required to ensure precision and accuracy fine enough to yield good results yet coarse enough to allow the integrals and iterations to converge.

#### REFERENCES

- Barge, P., Millet, J., & Pellat, R. 1984, ApJ, 284, 817  
 Barghouty, A. F., & Jokipii, J. R. 1996, ApJ, 470, 858  
 Batchelor, G. K. 1953, *The Theory of Homogeneous Turbulence* (Cambridge: Cambridge Univ. Press)  
 Bieber, J. W., Matthaeus, W. H., Smith, C. W., Wanner, W., Kallenrode, M.-B., & Wibberenz, G. 1994, ApJ, 420, 294  
 Bieber, J. W., Wanner, W., & Matthaeus, W. H. 1996, J. Geophys. Res., 101, 2511  
 Cane, H. V., Richardson, I. G., von Rosenvinge, T. T., & Wibberenz, G. 1994, J. Geophys. Res., 99, 21429  
 Cane, H. V., Wibberenz, G., Richardson, I. G., & von Rosenvinge, T. T. 1999, Geophys. Res. Lett., 26, 565  
 Chandran, B. D. G. 2000, ApJ, 529, 513  
 Corsin, S. 1959, in *Advances in Geophysics, Volume 6: Atmospheric Diffusion and Air Pollution*, ed. F. Frenkel & P. Sheppard (New York: Academic), 161  
 Erdős, G., Balogh, A., & Kóta, J. 1997, Adv. Space Res., 19, 843  
 ———. 1999, in *Plasma Turbulence and Energetic Particles in Astrophysics*, ed. M. Ostrowski & R. Schlickeiser (Kraków: Univ. Jagiellonski), 161  
 Fisk, L. A. 1996, J. Geophys. Res., 101, 15547  
 Giacalone, J., Jokipii, J. R., & Mazur, J. E. 2000, ApJ, 532, L75  
 Goldreich, P., & Sridhar, S. 1997, ApJ, 485, 680  
 Gray, P. C., Pontius, D. H., Jr., & Matthaeus, W. H. 1996, Geophys. Res. Lett., 23, 965  
 Isichenko, M. B. 1991a, Plasma Phys. Controlled Fusion, 33, 795  
 ———. 1991b, Plasma Phys. Controlled Fusion, 33, 809  
 Jokipii, J. R. 1966, ApJ, 146, 480  
 ———. 1973, ApJ, 183, 1029  
 ———. 1987, ApJ, 313, 842  
 Jokipii, J. R., & Coleman, P. J. 1968, J. Geophys. Res., 73, 5495  
 Jokipii, J. R., Kóta, J., & Giacalone, J. 1993, Geophys. Res. Lett., 20, 1759  
 Jokipii, J. R., & Parker, E. N. 1968, Phys. Rev. Lett., 21, 44  
 ———. 1969, ApJ, 155, 777  
 Jones, F. C., Jokipii, J. R., & Baring, M. G. 1998, ApJ, 509, 238  
 Kadomtsev, B. B., & Pogutse, O. P. 1979, in *Plasma Physics and Controlled Nuclear Fusion Research, Proc. 7th Int. Conf. (Vienna: IAEA)*, 649  
 Kirk, J. G., Duffy, P., & Gallant, Y. A. 1996, A&A, 314, 1010  
 Kóta, J., & Jokipii, J. R. 1995, Science, 268, 1024  
 Krommes, J. A. 1978, Prog. Theor. Phys. Suppl., 64, 137  
 Kunow, H., et al. 1995, Space Sci. Rev., 72, 397  
 Lithwick, Y., & Goldreich, P. 2001, ApJ, 562, 279  
 Maron, J., Chandran, B. D. G., & Blackman, E. 2004, Phys. Rev. Lett., 92, 045001  
 Matthaeus, W. H., & Goldstein, M. L. 1982, J. Geophys. Res., 87, 6011  
 Matthaeus, W. H., Goldstein, M. L., & Roberts, D. A. 1990, J. Geophys. Res., 95, 20673  
 Matthaeus, W. H., Gray, P. C., Pontius, D. H., Jr., & Bieber, J. W. 1995, Phys. Rev. Lett., 75, 2136  
 Matthaeus, W. H., Smith, C. W., & Bieber, J. W. 1999, in AIP Conf. Proc. 471, *Solar Wind Nine*, ed. S. Habbal, R. Esser, J. V. Hollweg, & P. A. Isenberg (Woodbury: AIP), 511  
 Mazur, J. E., Mason, G. M., Dwyer, J. R., Giacalone, J., Jokipii, J. R., & Stone, E. C. 2000, ApJ, 532, L79  
 McComb, W. D. 1990, *The Physics of Fluid Turbulence* (Oxford: Clarendon)  
 McKibben, R. B., Simpson, J. A., Zhang, M., Bame, S., & Balogh, A. 1995, Space Sci. Rev., 72, 403  
 Moraal, H. 1976, Space Sci. Rev., 19, 845  
 Parker, E. N. 1965, Planet. Space Sci., 13, 9  
 Press, W. H., Teukolsky, S. A., Vetterling, W. T., & Flannery, B. P. 1992, *Numerical Recipes in FORTRAN: The Art of Scientific Computing* (Cambridge: Cambridge Univ. Press)  
 Rax, J. M., & White, R. B. 1992, Phys. Rev. Lett., 68, 1523  
 Rechester, A. B., & Rosenbluth, M. M. 1978, Phys. Rev. Lett., 40, 38  
 Reinecke, J. P. L., McDonald, F. B., & Moraal, H. 2000, J. Geophys. Res., 105, 27439  
 Ruffolo, D., Matthaeus, W. H., & Chuychai, P. 2003, ApJ, 597, L169  
 Sagdeev, R. Z., Usikov, D. A., & Zaslavsky, G. M. 1988, *Nonlinear Physics: From the Pendulum to Turbulence and Chaos* (Chur: Harwood)  
 Salu, Y., & Montgomery, D. C. 1977, Phys. Fluids, 20, 1  
 Sanderson, T. R., Marsden, R. G., Wenzel, K.-P., Balogh, A., Forsyth, R. J., & Goldstein, B. E. 1995, Space Sci. Rev., 72, 291  
 Similon, P. L., & Sudan, R. N. 1989, ApJ, 336, 442  
 Simnett, G. M., Sayle, K. A., Tappin, S. J., & Roelof, E. C. 1995, Space Sci. Rev., 72, 327  
 Simpson, J. A., et al. 1995, Science, 268, 1019  
 Skilling, J., McIvor, I., & Holmes, J. A. 1974, MNRAS, 167, 87P  
 Zaslavsky, G. M., & Chirikov, B. V. 1972, Soviet Phys.—Uspekhi, 14, 549  
 Zimbardo, G., Veltri, P., & Malara, F. 1984, J. Plasma Phys., 32, 141